CHARACTERIZATION OF ALUMINA TITANIA CARBON NANOTUBE COMPOSITE PREPARED BY POWDER METALLURGY METHOD

NUR NAZIHAH BINTI NORDIN

FACULTY OF EARTH SCIENCE
UNIVERSITI MALAYSIA KELANTAN

2017

CHARACTERIZATION OF ALUMINA TITANIA CARBON NANOTUBE COMPOSITE PREPARED BY POWDER METALLURGY METHOD

by

NUR NAZIHAH BINTI NORDIN

A thesis submitted in fulfillment of the requirements for the degree of Bachelor of Applied Science (Materials Technology) with honour

FACULTY OF EARTH SCIENCE
UNIVERSITI MALAYSIA KELANTAN

2017

DECLARATION

I hereby declare that the work embodied in this report is the result of the original research and has not been submitted for a higher degree to any universities or institutions.

_____

Student

Name: **Nur Nazihah Binti Nordin**

Date: **29 December 2016**

I certify that the Report of this final year project entitled "Characterization of Alumina Titania Carbon Nanotube Composite Prepared by Powder Metallurgy Method" by Nur Nazihah Binti Nordin, matric number E13A218 has been examined and all the correction recommended by examiners have been done for the degree of Bachelor of Applied Science (Material Technology) with Honours, Faculty of Earth Science, Universiti Malaysia Kelantan.

Approved by:_____

Signature of supervisor

Name: **Dr. Mohamad Najmi Masri**

Date: **29 December 2016**

ACKNOWLEDGEMENT

In the name of Allah SWT, the Most Gracious and the Most Merciful, I offer my humble than gratitude You for giving me the strength to complete this thesis.

First and foremost, my sincere gratitude and appreciation goes to my supervisors, Dr Mohamad Najmi Masri, for his supervision and constant support. His invaluable help of constructive comments and suggestions throughout the experimental and thesis works have contributed to the success of this research. Not forgotten, my appreciation to my co-supervisor, Dr Mahani Yusoff for his support and knowledge regarding this topic.

I would like to express my appreciation to the Dean, Faculty of Earth Science, Prof. Assoc. Aweng A/L Eh Rak for his support and helps toward my undergraduate affairs. My acknowledgment also goes to all the lab assistants and office staffs of Faculty of Earth Science for their cooperation.

Sincere thanks to my entire friend especially Asma, Mim Rusyahida, , Izzaty Inu, Amirul, Huda, Adibah, Yus, Wardah, Dayana, Atieefah and Fariz for their kindness and moral support during my study. Apart from that, thanks to final year project team (Suliana, Adillah, Syuhada Adibah, Marinah, and Shahira) that had stayed together as a team throughout the final year project. Thank for the friendship and memories.

I wish to remember to my beloved late brother, Mohd Rildwan Nordin who was instrumental in this accomplishment and desired me to be success woman that will help others people around me especially our parent. My greatest pleasure would be share this moment with him.

Last but not least, my deepest gratitude goes to my beloved parent; Mr. Nordin Bin Hussin and Mrs. Rusiah Binti Draman and also to all my brothers (Hisan, Hasmadi, Syakir and Mushisyam) and sisters (Hazlina, Safiah, Farahani Nadia, Zalina, Haslila, and Wahida) for their endless love, prayers and encouragement. To those who indirectly contributed in this research, your kindness means a lot to me. Thank you very much.

Characterization of Alumina Titania Carbon Nanotube Composite Prepared by Powder Metallurgy Method

ABSTRACT

The present work investigates the characterization of alumina titania carbon nanotube (Al_2O_3–TiO_2–CNT) composite prepared by powder metallurgy (PM). The properties of Al_2O_3-TiO_2 composite have high hardness, chemical and thermal resistance, wear and corrosion resistance. This made Al_2O_3–TiO_2 composite used in various applications. However, Al_2O_3–TiO_2 composite have lack due to low fracture toughness and brittle. To overcome the problem, CNT was reinforced into Al_2O_3–TiO_2. CNT are most suitable material as reinforcement due to attractive mechanical properties, low density and high fracture toughness. Elemental powders of Al_2O_3, TiO_2 and CNT were milled in a low energy ball mill using different milling time at 15, 30, 45 and 60 h with 10 mm ball size. Then, the powder was compacted at different pressure at 200, 400, 600 and 800 MPa. The peak XRD of TiO_2 and CNT become diminished with increasing milling time. The powder that milled at 60 h has lowest crystallite size and highest internal strain due to finer and homogenous particle size deform during milling. The microstructure of particle size milled powder become smaller and finer with increasing milling time. Apart from that, after compaction, 45 h of milled powder have highest green density and densification parameter with increasing the compaction pressure from 200 to 800 MPa. This due to small particle of TiO_2 and CNT become diffuse into void of Al_2O_3 matrix. Thus,Al_2O_3–TiO_2–CNT composite have low porosity and increase in fracture toughness.

Pencirian Alumina Titania Karbon Nano Tiub Disediakan Menggunakan Metalurgi Serbuk

ABSTRAK

Kajian ini mengkaji pencirian alumina titania karbon nano tiub (Al_2O_3–TiO_2–CNT) disediakan menggunakan metalurgi serbuk (PM). Sifat-sifat Al_2O_3-TiO_2 komposit mempunyai kekerasan yang tinggi, rintangan kimia dan haba, haus dan rintangan kakisan. Ini menjadikan Al_2O_3-TiO_2 komposit digunakan meluas dalam pelbagai aplikasi. Walaubagaimanapun, Al_2O_3-TiO_2 komposit mempunyai kekurangan disebabkan oleh keliatan patah yang rendah dan rapuh. Untuk mengatasi masalah ini, CNT dimasukkan ke dalam sistem Al_2O_3-TiO_2. CNT merupakan bahan paling sesuai sebagai pengukuh disebabkan mempunyai sifat-sifat mekanikal yang menarik, ketumpatan yang rendah dan keliatan patah yang tinggi. Unsur- unsur serbuk Al_2O_3, TiO_2 dan CNT dikisar menggunakan bebola pengisar yang bertenaga rendah mengunakan masa mengisar yang berbeza pada 15, 30, 45 dan 60 jam dengan bola bersaiz 10 mm. Kemudian, campuran serbuk dimampatkan pada tekanan berbeza iaitu pada 200, 400, 600 dan 800 MPa. Puncak XRD bagi TiO_2 dan CNT menjadi berkurang dengan penambahan masa pengisaran. Serbuk yang dikisar pada 60 jam mempunyai saiz kumin hablur yang paling rendah dan tarikan dalaman tertinggi kerana lebih halus dan saiz zarah yang seragam terbentuk semasa pengisaran. Saiz zarah bagi serbuk yang dikisar semakin kecil dan lebih halus dengan penambahan masa pengisaran. Selain itu, selepas pemampatan, serbuk yang dikisar pada 45 jam mempunyai mampatan tertinggi dengan peningkatan tekanan pemadatan dari 200 hingga 800 MPa. Ini disebabkan oleh zarah kecil TiO_2 dan CNT meresap dalam lubang-lubang matrik Al_2O_3. Oleh itu Al_2O_3–TiO_2–CNT komposit mempunyai liang yang kecil dan berlaku peningkatan dalam keliatan patah.

TABLE OF CONTENT

CHAPTER 2 – LITERATURE REVIEW

CHAPTER 3- MATERIALS AND METHODOLOGY

LIST OF TABLE

LIST OF FIGURES

LIST OF ABBREVIATIONS

Al_2O_3	Alumina
BET	Brunauer Emmett Teller
CMC	Ceramic Matrix Composite
CNT	Carbon Nanotube
CVI	Chemical Vapour Infiltration
FWHM	Full Width Half Maximum
GD	Green Density
HP	Hot Press
MMC	Metal Matrix Composite
MA	Mechanical Alloying
PM	Powder Metallurgy
PMC	Polymer Matrix Composite
SEM	Scanning Electron Microscope
SG	Sol Gel
SPS	Spark Plasma Sintering
SrO	Strontia
TEM	Tranmission Electron Microscope
TiO_2	Titania
WH	William Hallson
XRD	X-Ray Diffraction
ZrO_2	Zirconia

LIST OF SYMBOLS

h	Hours
g	Gram
cm	Centimetre
MPa	Mega Pascal
cps	Count per second
wt%	Weight percent
nm	Nano metre
mm	Millimetre
µm	Micrometre
GPa	Giga Pascal
ºC	temperature
º	Degree
rpm	Rotate per minute
λ	Lambda
%	Percentage
B_r	overall broadening
Å	ÄngstrÖm
B_i	Instrumental broadening
B_o	Sum of the total broadening of size, lattice strain and instrument
k	Constant
B_{strain}	Broadening due to strain
B_{cryst}	Broadening due to crystallite size

m	Mass
V	Volume

CHAPTER 1

INTRODUCTION

1.1 Background of Study

Composites will be defined as one or more discontinuous phases embedded in a continuous phase on macro scale that can improve the properties of material (Banga et al., 2015; Gupta, 2014). The discontinuous phase are called reinforcement is usually harder and stronger than the continuous phase that are called as matrix. Composite will be divided into three classifications which are metal matrix composite (MMC), polymer matrix composite (PMC) and ceramic matrix composite (CMC).

CMC is material that promises as potential candidates in view of excellent physical and mechanical properties. This is due to their properties like high temperature stability, chemical inertness, strength and corrosion resistance that appropriate usage in industry (Zahedi et al., 2015; Zhao, 2014). In previous years, many researchers have been carried out to produce CMC in advance material that used in various industries such as electrical (Sekino and Niihara, 1997), medical application (Callister, 2011; Zapata et al., 2012; Kora et al., 2006; Miura, 2014) aerospace and automotive part (Zapata et al., 2012; Kanthavel et al., 2016; Yan and Wei, 2014).

Alumina (Al_2O_3) ceramic material is mostly used as matrix for CMC application because of their superb properties such as high hardness, high compressive strength (0.5-5.0 wt.%) and good chemical resistance (Kora et al., 2006; Palmero et al., 2014; Rangel et al, 2014). This was proved according to many of CMC that applied of Al_2O_3 based ceramic as matrix material. For example, Al_2O_3

based silver (Al_2O_3–Ag) that improve fracture toughness in range 3.2 MPa·$m^{1/2}$ (Rangel et al., 2014) and Al_2O_3 based silicon carbide (Al_2O_3−SiC) (Erdemir et al., 2015).

Based on research that was reported by Bian et al. (2012), alumina–titania (Al_2O_3-TiO_2) is one of CMC that already fascinating study by others due to good ceramic material for many applications such as machinery, textile and printing industries. Al_2O_3-TiO_2 also has tremendous properties due to their high hardness, excellent wear corrosion, chemical and thermal resistance (Dubourg et al., 2007; Sakka et al, 2014). However, Al_2O_3-TiO_2 composite have limitation leading to poorer fracture toughness and high porosity because of not fully homogeneous of the grain size.

In order to improve the properties of Al_2O_3-TiO_2 composite, carbon nanotube (CNT) will be added to become Al_2O_3-TiO_2 systems prepared by powder metallurgy (PM) technique. CNT play an important role in order to improve the Al_2O_3-TiO_2 composite because of extent excellent properties such as high tensile strength in range of 10−100 times greater than steel (He et al., 2015), low density (~2.1 g/cm^3) (Yavas et al., 2015), light weight, promising stiffness, Young's modulus (973 GPa) (Kondoh et al., 2008) and high strength (up to ~100 GPa) (Chen et al., 2015; Esawi et al, 2010).

On the other hand, CNT also provide excellent reinforcement as composite due to many potentials used in application. For examples, it was used in automotive, aircraft and sport industries (Esawi et al., 2010; Jagannatham et al., 2015; Li et al., 2016). The interest to apply this material regarding to light weight and low density properties (Esawi et al., 2010).

The are many way to fabricate the composite such as rotating cube, precise casting, sol gel (SG), spark plasma sintering (SPS), forging and powder metallurgy (PM) (Dehaghani et al., 2014). In powder processing, SG and SPS method is widely used as casting processing. In SPS, the consolidation of powder compacts is carried out at low sintering temperature with short time to escape grain growth and have unwanted chemical reaction occurred (Jagannatham et al., 2015). However PM is the best way to fabricate the composite due to their ability to produce design that have limitation by other method.

PM can be defined as material processing technique used to consolidate particulate matter either powder both metal or non metal (German, 1997). PM is a method that almost produce material that promising the customers requirement. PM also important technique because it an alternative and economically viable mass production for structural component to very close tolerance (German, 1997). Moreover, PM can produce some parts that cannot be provide by other available methods. The imperative points of interest in PM over other throwing methods incorporate the uniform dispersion of fortifying particles inside the network and less failure because of lower handling temperatures (Abdizadeh et al., 2011; Pournaderi et al., 2012).

The major processing in PM fabrication technique consists of three steps. First, the mixing powder elements, follow by compacting those powder elements in a die at room temperature. Then, heating in a controlled atmosphere furnace to create a bond between the powder elements as called as sintering process (Nassar and Nassar, 2015; Sabzevari et al, 2015).

1.2 Problem Statement

Most studies on the fabrication of $Al_2O_3 - TiO_2$ ceramic composite that use powder metallurgy method recently were discovered and explored by previous researchers (Furlani et al, 2014; Rahimian et al., 2010; Rout, 2013). Accordingly, Al_2O_3-TiO_2 has outstanding properties that widely suitable used in high performance application such as high hardness, excellent wear, corrosion, chemical and thermal resistance. Nevertheless $Al_2O_3 - TiO_2$ still have limitation due to low fracture toughness and brittle. This due to Al_2O_3 not fully homogenous when mixed with TiO_2 (Inam, 2009).

Moreover, in preliminary work, there are many examples of reinforcement used to mix with Al_2O_3 in order to improve their limitation due to low fracture toughness (Oungkulsolmongkol., 2010). For example Strontia (SrO) that increasing in fracture toughness for the first when added 5% of SrO but slightly continuously decreased the fracture toughness when heat at certain temperature (Oungkulsolmongkol et al., 2010). In fact, Mishra et al. (2014) discovered that boride phases was embedded in Al_2O_3 to improve mechanical properties.

In this work, CNT will be added as reinforcement to improve properties of Al_2O_3-TiO_2 composite. CNT are most suitable material as reinforcement due to their attractive mechanical properties, large aspect ratio and low density (Esawi et al., 2010). It can also be improved the composite at optimize milling time and compaction pressure using powder metallurgy method. Based on study by Yavas et al. (2015), found out that fracture toughness of B_4C increase to 5.94MPa $m^{1/2}$ by adding 3 wt. % CNT. Last but not least, the ability of CNT as filler that will improve the properties of Al_2O_3-TiO_2 composite will be discovered.

1.3 Objective

The objectives of this work are:

i. To study the effect of milling time on structural and microstructural properties of Al_2O_3-TiO_2-CNT composite.

ii. To evaluate the effect of compaction pressure on Al_2O_3-TiO_2-CNT composite prepared by PM.

1.4 Scope of Study

The important of this research was to study the effect of Al_2O_3-TiO_2-CNT composite that fabricated by powder metallurgy. It based on characterization of structural and microstructural properties when conduct at difference milling time and compaction pressure. The microstructures of Al_2O_3-TiO_2-CNT will be fully homogenous distribution without agglomeration between combinations of reinforcement and matrix prepared by PM method. The structural will produce CMC that high toughness and ductility that will be used in various applications such as in medical field, automotive, cutting tool and construction.

CHAPTER 2

LITERATURE REVIEW

2.1 Introduction

The processing and properties of ceramic matrix composite (CMC) mainly for Al_2O_3 as a matrix was briefly discussed in this chapter. The preparation methods of CMC are used such as powder metallurgy (PM), sol gel (SG) and others. Besides, the characterization of CMC also was explained based on previous research for CMC.

2.2 Ceramic Matrix Composite

Ceramic is one material that currently applied in many field because of its properties that basically used as a matrix in composite. Ceramic matrix composite (CMC) materials have been improved extensively the fracture toughness in range of 6 to 20 MPa by development of CMC in particulate, fibres or whisker orientation that embedded into matrix (Callister, 2011). Low (2014), reported that the combination of reinforcing ceramic with other material will achieve excellent properties of material such as strong, tougher structure, and temperature stability.

There are main methods that prominent used to manufacture of CMC material, such as hot pressing (HP), chemical vapour infiltration (CVI), Sol gel (SG) and powder metallurgy (PM) (Deborah, 2010; Callister, 2011). CMC material broadly utilized as a part of various applications because of light weight and hardness properties (Zainudin and Sapuan, 2009).

CMC be intensive material that was remarkable used in huge application such as in medical field as a dental implant and hip prostheses that basically used ceramic like zirconia (ZrO_2) and Al_2O_3 (Rout, 2013). Based on others research, CMC material are demanding in aerospace field for application such as turbine blade, combustor and nozzle (Ohnabe et al., 1999; Zeng et al., 2013; Zhao, 2014).

2.2.1 Matrix

According to Thomas et al. (2012) the matrix phase is a phase that having a continuous character and usually it is more ductile and less hard phase. It also can be defined as material that gave body structure to the composites (Al-bahadly, 2013). The matrix phase is important to hold the reinforcement material together by surface connection. However, matrix is low strength compared to reinforcement material.

There are many types of ceramic that was usually used as matrix in composite. Two classification of advance ceramic as a matrix which are oxide ceramic and non-oxide ceramic (Callister, 2011). There are large attract in CMC for various matrix in composite such as silicon carbide (SiC), alumina (Al_2O_3), boron carbide (B_4C), titanium carbide (TiC), titania (TiO_2), zirconia (ZrO_2) and silicon nitride (Si_3N_4). The materials have been exploited because of their tremendous properties (Deborah, 2010).

β-tricalcium phosphate (β-$Ca_3(PO_4)_2$)(β-TCP) also common consideration as matrix because of its extraordinary natural reactions to physiological environment (Sakka et al., 2014). ZrO_2 also will be category as potential ceramic material that responsible as matrix in CMC for aerospace applications at high temperatures due to very refractory compound (T_m 2700°C), stable oxide, good insulating material

(Minet et al., 1990; Zahedi et al., 2015). Nevertheless, these materials are expensive and need special apparatus in preparation.

Among the materials state, Al_2O_3 is the most interested in recent research. Al_2O_3 is broadly considerable as matrix in composite that used in huge application in wide world. Al_2O_3 is more suitable compare to others ceramic in application of automotive and aircraft due to light weight and low density (Rahimian et al., 2010; Yang et al., 2009). However, Al_2O_3 still have limitation due to low fracture toughness and brittle that need to improve by add reinforcement (Inam, 2009; Palmero et al., 2014; Sakka et al., 2014).

2.2.2 Reinforcement

Reinforcement is used in composite to improve or enhances the properties of composite material. There is an expanding need worldwide for the progressed materials with a specific end goal to acquire the desired properties. This is because a single material generally cannot meet the requirements of extreme engineering environments. The properties of reinforcement material are novel with respect to use in different applications.

According to An et al. (2015), densification of composite are also influence by reinforcement particle size. In fact, reinforcement particle-to-matrix powder size ratio (Rs/Ms) determines the densification behavior of CMC as the reinforcement particle size was remaining constant. Hence, this will increase the density with increase of reinforcement ratio per matrix (An et al., 2015).

Based on research by Sanjay et al. (2015), the reinforcing phase material may be in the form of fibers, particles or flake that will provide different properties of composites. As stated by Callister (2011), carbon nanotube (CNT) is one material that have properties that exceptionally promise as a reinforcement in composite material. Moreover, the combination between CNT with other ceramic materias because of a high aspect ratio, excellent stiffness and strength will provided prominent for reinforcing a large spectrum of materials (Zahedi et al., 2015). CNT is also be responsible as a filler to improve the composite material.

2.3 Processing of Ceramic Matrix Composite

There are common techniques that have been adopted to prepare CMC that are developing in recent years. In this subtopic, the several methods were discussed due to process and applicable used. A detail description of several method such as PM, sol gel (SG), spark plasma sintering (SPS) and chemical vapor infiltration (CVI) was discussed. Nonetheless, PM was selected as method to prepare the CMC in this word.

2.3.1 Sol Gel

Sol gel (SG) involves the use of a hydrolysis reaction to obtain a cross-linked network, which results in the formation of a gel. SG processing methods provide an attractive and alternative route to generate a homogeneous and well-distributed dispersion of CNT throughout a ceramic matrix due to involves the production of a sol containing ceramic particles, where in CNT are mixed and entrapped in the gel network (Zapata et al., 2012).

According to Nenova et al. (2016) the SG method is a versatile method that enables development of entire new generations of composite materials. Apart from the homogenization of composite will achieved during impregnation by lowering temperature because small particle size compare to slurry infiltration (Deborah, 2010). Based on study by Somani (2006), there have some advantages of synthesis of material by SG method such as:

i. low temperature synthesis
ii. ease in controlling composition variations
iii. inexpensive

However, SG method still has weakness due to unnecessary shrinkage during heat treatment of composite (Deborah, 2010). This is due to uncontrol reaction during elevated temperature. Thus, the desired dimension of endproduct composite cannot be the control.

2.3.2 Spark Plasma Sintering

SPS is a novel sintering technique for the densification of CMC and will be achieved at lower temperature compare with other method due to passing heat through a graphite die by high pulsed direct current and the sample need to sinter at elevated temperature (Huang and Nayak, 2014). The SPS process heats the powder compact directly by the pulse arc discharges, thus achieving very high thermal efficiency (Low, 2014).

Moreover SPS also will be used after the green compaction for consolidation of the mixed powder (Ogawa and Masuda, 2015). Besides, by using SPS, compacts of powder show superior strength and uniform composition compared to the characteristics possible with many other manufacturing processes (Miura, 2014).

SPS is one method that appropriate to prepare CMC that are generally known as porous material that have limitation due to their brittleness and low flaw tolerance. Figure 2.1 demonstrates the schematic diagram of SPS method. The scope of exploration has been completed into designing porous ceramics with great mechanical properties with utilizing SPS method incorporate laser by pulse electric current sintering that promising technique for fabricating porous ceramics with enhanced mechanical properties (Yang et al., 2009).

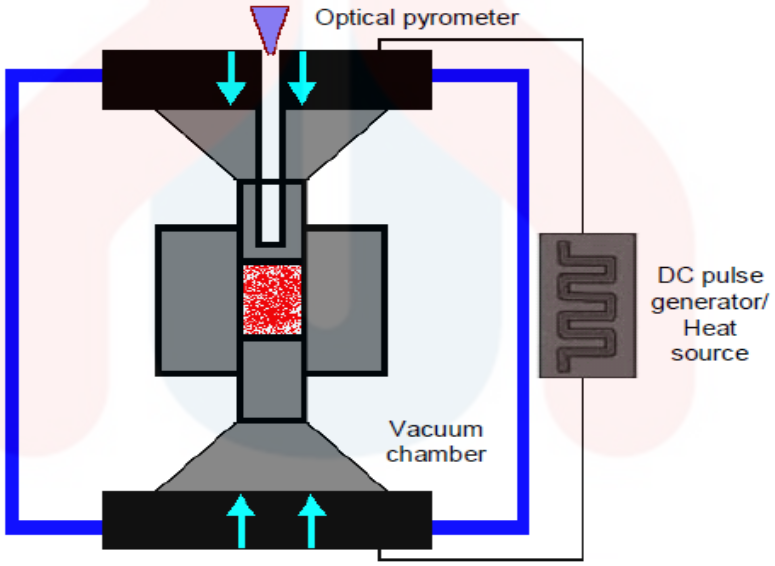

Figure 2.1: Experiment setup for SPS (Inam, 2009)

2.3.3 Chemical Vapor Infiltration

CVI is a method that process at high temperature in between 700-2000 $^{\circ}$C in the present of gas phase impregnation of hydrocarbon gas such as methane into carbon fibre to produce pyrolytic carbon by deposited gas in the open pore (Deborah, 2010). In addition, CVI is a method that allows the deposition of new phases by the transport of gas precursors through a porous ceramic body, that known as the

preform. CVI is a process that used for form composite or product from porous material like ceramic to produce porous structure that illustrates in Figure. 2.2.

Flores et al. (2012) CVI route was used in a multi step approach to synthesize micron-sized and nano-sized Si_3N_4/Si_2N_2O reinforcements into Si particulate preforms to produce produce $Si/Si_3N_4/Si_2N_2O$ porous composites. Thus, the compact deposits conservative stores and nanoweb morphology dispersed well into the composites that increment ~43% the $Si/Si_3N_4/Si_2N_2O$ porous composites after the handling.

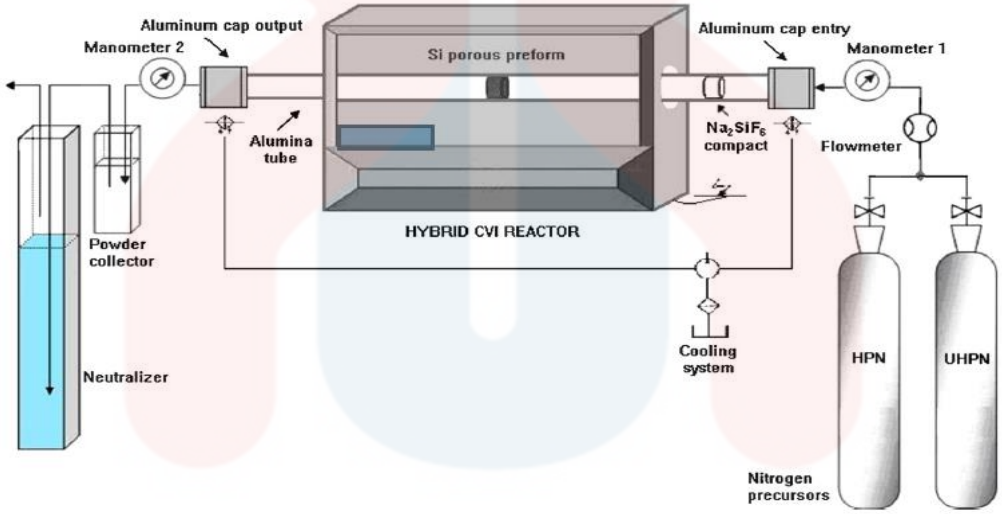

Figure 2.2: The schematic diagram of process set-up (Flores et al., 2012)

The main advantages of CVI are requirement for application that need thermal stability, temperature stability, excellent thermal shock resistance and resistance to chemical attack (Aguilar et al., 2013). While, the drawback of CVI method is low rate of deposition when used of low gas pressure (1-150 Torr) that long time for reactant and decomposed gases and also need for high cost (Deborah, 2010).

2.3.4 Powder Metallurgy

PM technique is chemically precipitated powder and new consolidation of material without used high temperature. While, on 1940's PM method more improve due to major growth used that tailor composition for nuclear, aerospace, electrical, and magnetic application (German, 1997).

An et al. (2015) discovered that the powder innovation has been attractive in automotive and aviation commercial ventures over the past half-century. Keeping in mind, the end goal to deliver modern segments with high strength-to-weight, high ratio, high resistance to thermal stress and high wear resistance. Moreover, PM route is one of the most widely used methods for producing composite material due to its low processing costs as well as the ease of preparation. Besides, the accuracy to obtain near net shaped components of complex geometry will get. The most elemental step of PM technique are mixing of powders, compaction, and sintering (Fathy et al., 2015).

Milling is process that involve powder in the mechanical agitation used to break particles or agglomerates into smaller particles and mixing, which is the process of thorough incorporating of two or more powders (Lin and Shih, 2015). Milling or blending of powder one of method to homogenize the powder. These powders were blended uniformly to produce a powder mixture with composition of

Al_2O_3 and TiO_2 with the addition of binder by wet ball milling (Yang et al., 2008). The increasing milling time will increase the homogeneity of particle distribution and improved the tensile strength (Sabzevari et al., 2015). Furthermore, milling time also will affect the physical properties of the composite. Length of milling has a strong influence on in situ formation of second phase and structural and compositional refinement of the milled powder (Mahani, 2012).

As another point of view, compaction is one part of method to prepare the composite shape which involves converting the initial powder into dense and bulk material in a die. This also called as green compact. There are three type of compaction powder which is uniaxial, isotactic and hot pressing (Callister, 2011).

Conventional uniaxial powder compaction will be performed with the pressure applied along one axis using hard tooling of die and punches. It is the most widely used method to compact powders because of easier method and low cost processing (Lin and Shih, 2015). Figure 2.3 shows the schematic diagram of in uniaxial compaction pressing. While, different pressure of compaction will be affected the densification of composite powder that can caused the density of sample are dense and high ductility.

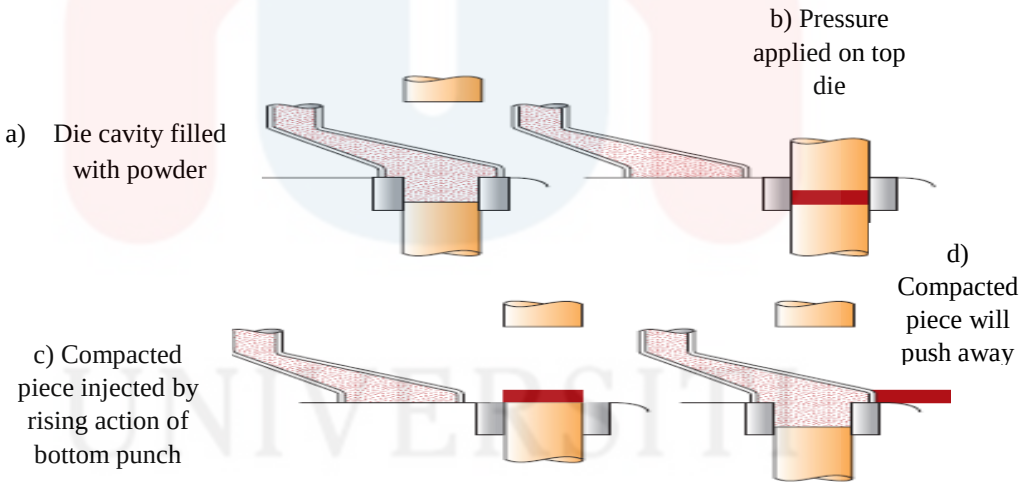

Figure 2.3: The schematic diagram of step in uniaxial compaction pressing

(Callister, 2011)

For isotactic pressing, the powder will be surround by rubber envelop and applied pressure by fluid, isostatically. However, this method cannot produce complicated shape compare to uniaxial technique and more expensive (Callister, 2011). Figure 2.4 shows a schematic of hot pressing using indirect resistance heating. Hot pressing is a method that applied high pressure, high temperature and low strain

rate synthesis process. These in order to form dense and compact material compared to cold press that be used for compact product at low pressure (Hu et al., 2014; Mahani and Zuhailawati, 2013).

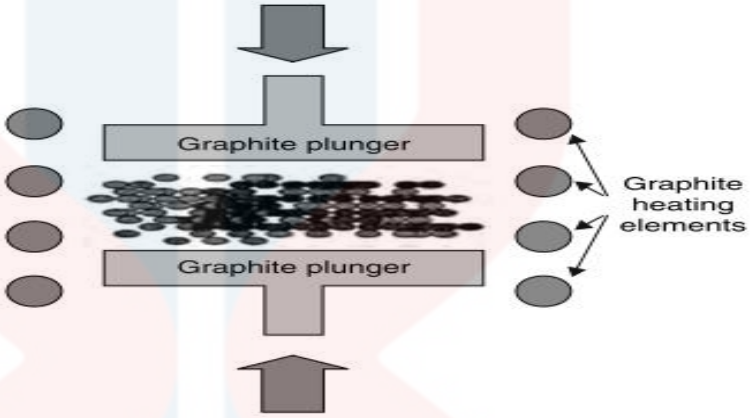

Figure 2.4: Hot pressing using indirect resistance heating (Hu et al., 2014)

Sintering was defined as process of consolidating either a loose arrangement of powder or a green compact of the desired composition under controlled condition of temperature and time. Thermal treatment of a powder or compact at a temperature below the melting point of the material also can be known as sintering. The compact sample is usually heated in protective atmosphere such as argon or hydrogen. Several changes take place during sintering like shrinkage, formation of solid solution and development of final microstructure (Thakur et al, 2007; Xiao et al, 2011).

During sintering, the bond of particles will be strength due to temperature of sintering. The pore of particles was change become sphere when sufficient temperature. According to Garg et al, (2007) and Palmero et al, (2014), the pore channel pinch off and close when sintered. A network of pores and a skeleton of solid particles are formed. In this stage, migration of the grain boundaries between the original particles by grain growth takes place.

The sample becomes shrinkage at this stage due to pore channel closure happen and the pores become isolated and are no longer interconnected between particles. Thus, this will show that sample has brittle properties due to crack or shrinkage at temperature used (Callister, 2011). The Figure 2.5 shows the changing microstructure pore of particle when sample was sintered at different temperature.

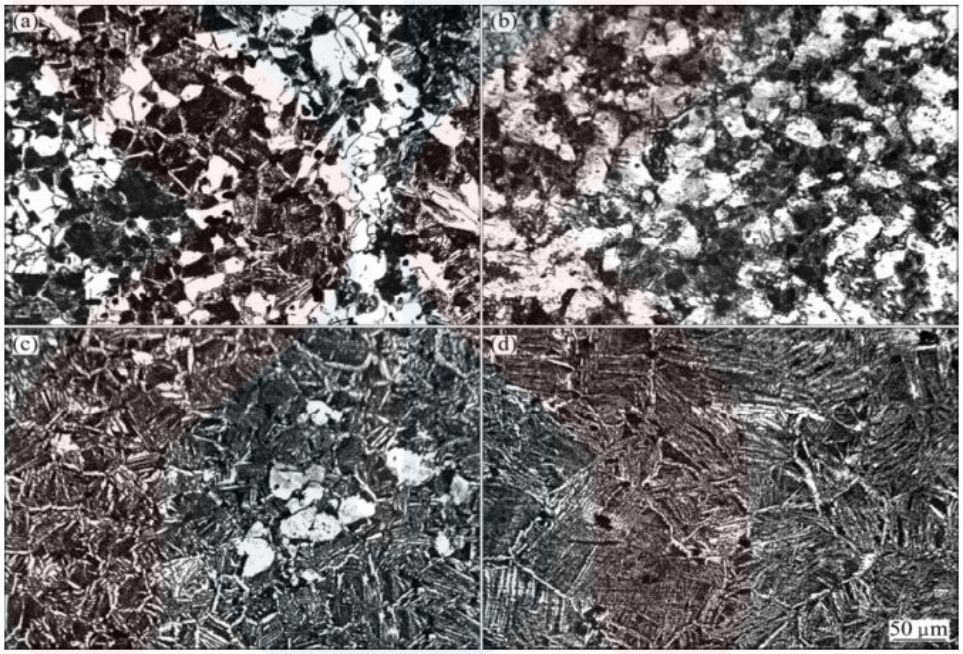

Figure 2.5: The change of optical microstructure of sample at different temperature of sintered (Xiao et al., 2011)

The process of sintering can be dividing into three stages that are shown in Figure 2.6. Necks are formed at the contact points between the particles of sample, which continue to grow at first stage. At initial stage, rapid creation of neck and neck growth was undergoing in the powder compact. While this stage, the pores are interconnected and the pore shapes are irregular. In the second stage of sintering, with sufficient neck growth, the pore channels become more cylindrical.

In sintering process, there have different type of sintering that widely used in industry such as solid state sintering, liquid phase sintering, activated sintering, rate controlled sintering, microwave sintering, gas plasma sintering and spark plasma sintering (Callister, 2011; Flores et al., 2012). Different type of sintering used depends on temperature and application of sample.

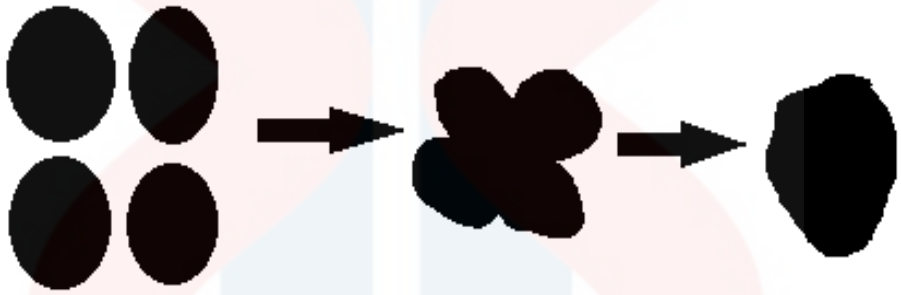

Figure 2.6: Three steps of sintering process

2.4 Alumina based Composite

Al_2O_3 is an oxide of aluminum, a group III element, well-known to be a very stable and robust material. Al_2O_3 (corumdum) has a hexagonal structure that is shown in Figure 2.7 (Somani, 2006). Besides, Al_2O_3 is one of the most widely used of advance ceramic in material industry that very important because of hard, high-temperature, excellent thermal stability and chemical inertness oxidation-resistant composites (Kora et al., 2006; Mishra et al., 2014; Mohseni et al., 2013). Moreover, Al_2O_3 also one type of ceramic that will also improve of high compressive strength based on Rocha et al. (2014) and unique mechanical, electrical, and optical properties (Yang et al., 2008).

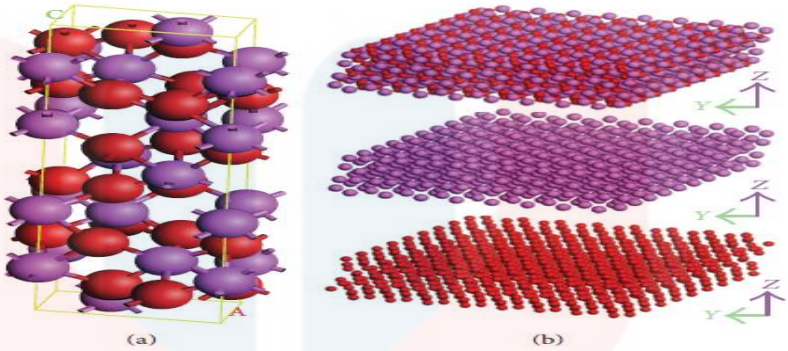

Figure 2.7: Crystal structure of α-alumina. (a) The crystal structure cell, a = 0.4759 nm, b= 0.4759 nm, b and c = 1.2991 nm; (b) the crystal structure of α-alumina, the oxygen atom cluster and aluminum atom cluster (Yan and Wei, 2014)

The utilization of alumina ceramics production in medicinal application like prosthetics and dental implants depends on the imperviousness to corrosion and Al_2O_3 additionally reasonable for utilized as prosthetic. For example, as a part of hip joint prostheses, high loads must be acknowledged over drawn out stretches of time on account of high resistance pressure (Somani, 2006).

The reinforcement in Al_2O_3 based composites can be in a form of particulates, whiskers, and short and long fibres (Oungkulsolmongkol, 2010). From the research by Yang et al. (2008) Al_2O_3 will promise the user for the application fields of refractory and engine components because of high melting point aspect that suitable for high temperature application.

Table 2.1 shows the summary of major properties of Al_2O_3 that made it will be used in various applications. Recently, Al_2O_3 likewise will for the most part be applicable immense utilized as a part of the aeroplane and automotive commercial industries due to light weight, superb in strength properties furthermore great sturdiness and thermos shock resistance that one of imperative properties of material

used as segment or a portion of aeroplane (Hackemann., 2010; Pournaderi et al., 2012) .

Table 2.1: General properties of Al_2O_3

Properties of Al_2O_3	
Density	3.4-3.7 gcm^{-3}
Thermal expansion coefficient	7.5-8.5×10^{-6} $^{\circ}C^{-1}$
Compressive strength	1000-2800 MPa
Tensile strength	140-170 MPa
Flexural strength	280-420 MPa
Wear strength	550-600 $Mpam^{-1}$
Fracture toughness	3-4 $MPam^{-1/2}$
Thermal conductivity	30-40 $Wm^{-1}K^{-1}$
Specific heat	880 $J.kg^{-1}K^{-1}$
Elastic modulus	350-400 GPa
Shear modulus	140-160 GPa
Bulk modulus	210-250 GPa
Microhardness (kN)	1400-1800 $kgmm^{-2}$
Dielectric strength	10-17$kV.mm^{-1}$
Dielectric permittivity	9.8 (1 MHz)
Volume resistivity (RT)	>1014 $ohmcm^{-1}$

2.5 Titania as Reinforcement Phase

TiO_2 can be found in three forms which are rutile, anatase, and brookite. The schematic diagram the octahedra-packing style of rutile and anatase has been showed in Figure 2.8. According to Kumar and Rajadurai (2016), rutile is the most abundant and thermodynamically is the most stable TiO_2 phase that common natural form of TiO_2 anatase and brookite will be transform into thermodynamic stable phase of rutile at high. In addition, it is promptly accessible, modest and holds significant

wear resistance, mechanical and thermal properties (Kumar and Rajadurai, 2016; Tahara et al., 2014; Yashwanth and Gurrappa, 2015).

TiO_2 has their unique properties, which are relatively with biological environment because of biocompatibility and biodegradation proportion that not harmful the human body (Somani, 2006). Apart from that, TiO_2 also used material in photocatalysts application (Wang et al., 2016; Maria et al., 2015; Nguyen et al., 2013) due to its excellent photocatalytic activity.

Besides, it is also has been used in other application such as cosmetics, gas sensors (Wang et al., 2016), self-cleaning coating (Maria et al., 2015; Nguyen et al., 2013), antibacterial coating on medical device (Wang et al., 2016; Maria et al., 2015; Nguyen et al., 2013), energy storage device (Maria et al., 2015), dye-sensitized solar cells (Maria et al., 2015) and photoelectric conversion in solar cell (Nguyen et al., 2013). This can be explained that TiO_2 is one material that suitable in many field of application due to the excellent properties and low cost material.

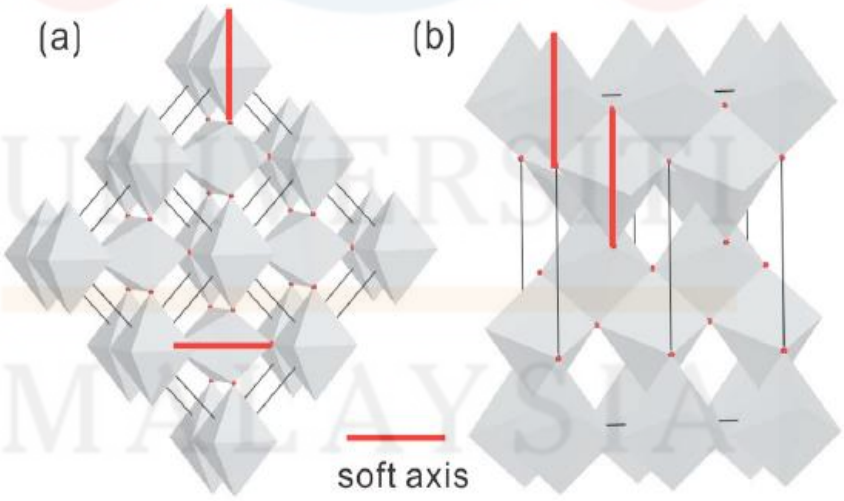

Figure 2.8: The octahedra-packing style of rutile (a) and (b) anatase TiO_2 (Yin et al., 2011)

In addition, TiO_2 is steady, safe and economical which likewise has incredible properties such as high effectiveness of photograph created electron, chemical intentness, photo erosion and chemical consumption (Chen et al., 2011). Figure 2.9 shows the example morphology of nano sized raw powders of TiO_2. The SEM image of TiO_2 revealed very small particle because size in nanometer that can easy reinforced with other matrix and provide high strength for composite.

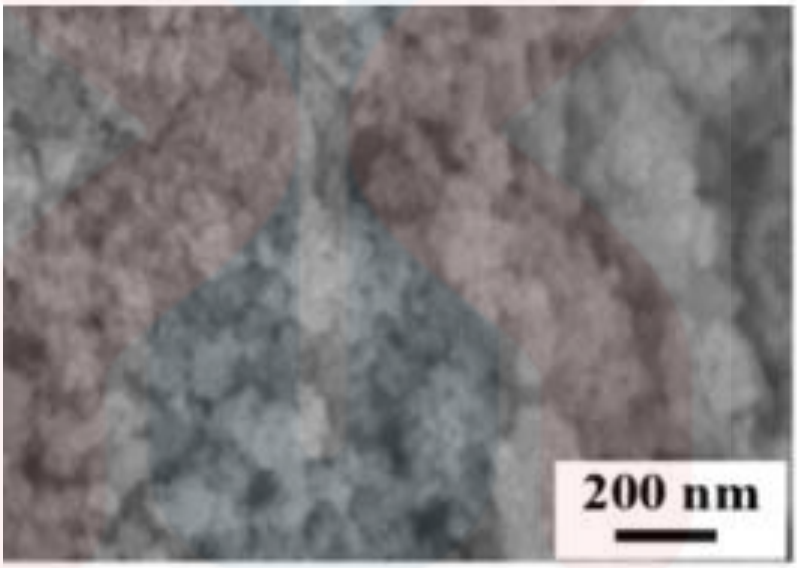

Figure 2.9: The SEM micrographs of nano-sized raw powder of TiO_2 (Bian et al., 2012)

2.6 Alumina Titania Based Composite

Alumina Titania (Al_2O_3–TiO_2) ceramic composite materials have been widely used as wear resistant coatings in machinery, textile and printing industries due to their high hardness, excellent wear, corrosion, chemical and thermal resistance (Bian et al., 2012). The addition of TiO_2 as a reinforcement in Al_2O_3 composites, because of improvement the fracture toughness and thermal shock resistant in alumina either

by the addition of second phase or by the microstructure designs such as duplex or duplex-bimodal heterogeneous and layer structures (Mohseni et al., 2013).

Sakka et al. (2014) found that TiO_2 has been added in Al_2O_3 as reinforcement that has been used in orthopedic applications because of excellent mechanical resistance, chemical stability in aqueous environments and its chemical inertness (Inam, 2009).

2.7 Carbon Nanotube as Filler

CNT were defined as carbon allotrope and cylindrical nanostructure. The different type of CNT structure has been detailed on Figure 2.10. CNT will be categorized by two difference types structure which is single wall carbon nanotube (SWCNT) and multi wall carbon nanotube (MWCNT). CNT can be conceptually visualized as rolled graphene.

The discovery of CNT by Iijima in the early 1990s, CNT have been the subject of intense research efforts aimed at characterizing and understanding their notable mechanical, electrical and thermal properties (Kumar et al., 2007). From the studied by Inam (2009), the main cylindrical part of CNT is like chicken wire, based on hexagons, whereas the end caps correspond to half a fullerene molecule, made of hexagons and pentagons. The classification of CNT are base on number of graphene cylinder, (x). (SWCNT, x=1) while (MWCNTs, x > 2).

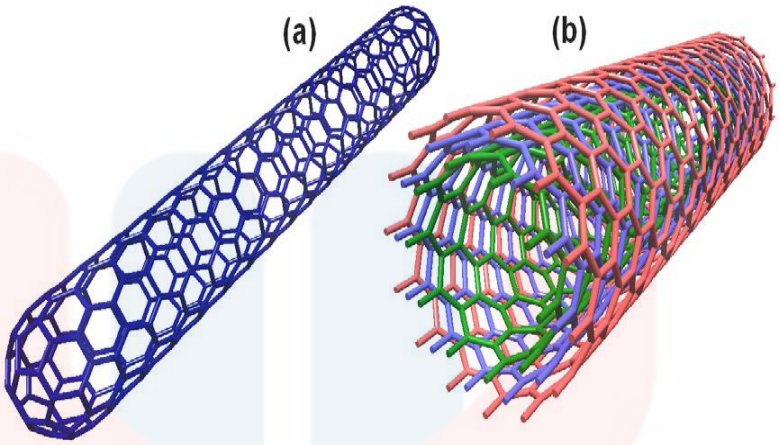

Figure 2.10: Different types of CNT based on their number of graphene cylinders: (a) SWNT; and (b) MWNT (Inam, 2009)

CNT is great material that can attract caption researcher to use it in various applications because of their excellent properties. High strength (up to ~100GPa), high Young's modulus (~1TPa) along with high aspect ratio(100-1000) and light weight (~2 g cm^{-3}), make CNT ideal reinforcements for structural composites (Chen et al., 2015; Esawi et al., 2010; He et al., 2015; Kondoh et al., 2008).

The aim added CNT in the various groups such as polymer, ceramic and metal because would make attractive novel materials with potential applications in the aerospace, automotive and sports industries where light weight combined with high stiffness and strength is desired (Esawi et al., 2010). Furthermore, CNT are also main material that are most chosen in industries field because of CNT are very promising reinforcements in composite materials for structural applications due to their attractive mechanical properties, large aspect ratio and low density (Jagannatham et al., 2015).

Regarding to Zeng et al. (2013) CNT also will raise the strength of matrix without lowering their toughness. The unique of characteristic of CNT such as sensitive to electrically made it suitable as semiconductor material. For example used as computer monitor and television screen (Callister, 2011). Inam (2009) concentrated on the impact of CNT substance on the tribological properties of Al_2O_3– CNT nanocomposites will lessen 56% in the wear and 30% improvement in the microharness of the nanocomposite were observed as compared to pure Al_2O_3.

2.8 Characterizations of Composite Product

The previous studies that involve the powder material to form composite, the characterization of milling and compaction powder was carried out. The phase analysis has been evaluated by X-ray diffraction (XRD) and the morphology of ceramic composite has been observed by scanning electron microscope (SEM).

2.8.1 Phase Analysis

Sakka et al. (2014) described the XRD pattern obtained from the alumina powder reveals the α phase peaks relative to corundum as Figure 2.11(a) while Figure 2.11(b) showed the XRD pattern of the TiO_2 powder shows only peaks of anatase. This shows the phase identification that present about the peak of Al_2O_3 and TiO_2.

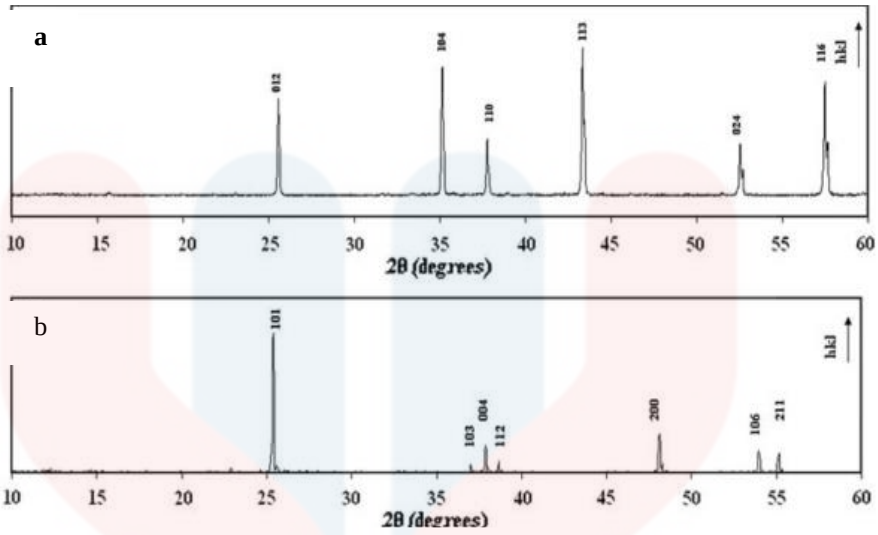

Figure 2.11: XRD pattern of different material; (a) Al_2O_3 and (b) anatase TiO_2

(Sakka et al., 2014)

Basically, the peak of Al_2O_3 has highest peak at range 30˚ to 40 of 2θ. Based on previous research the priority peak of TiO_2 present was indicate at range between 20˚ to 30˚ of 2θ (Bian et al., 2012; Meybodi et al., 2013; Mishra et al., 2014; Sakka et al., 2014). The XRD pattern of Al_2O_3-TiO_2 show the peak changed when powder was milled. Figure 2.12 represent the image XRD of Al_2O_3 -TiO_2.

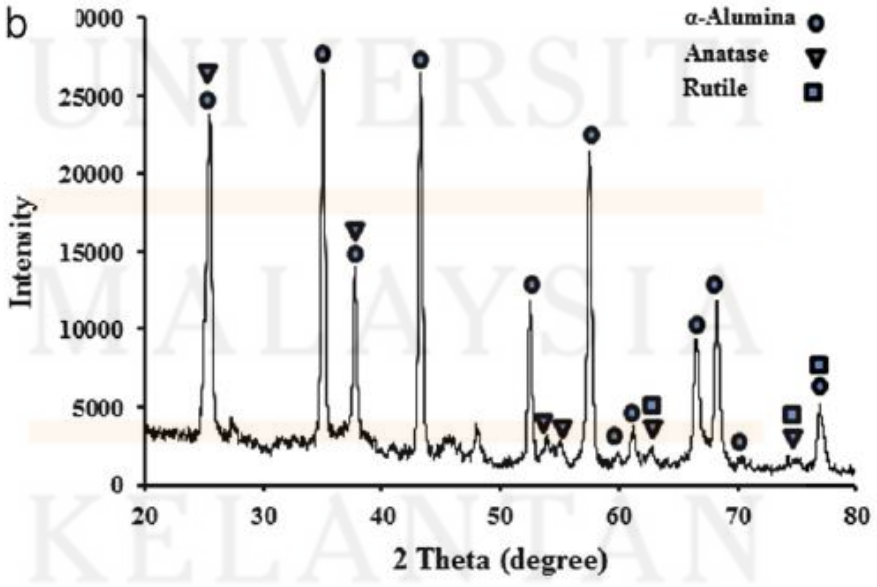

Figure 2.12: XRDpattern of Al2O3–TiO2 nanocomposite powder (Meybodi et al., 2013)

2.8.2 Morphology of Composite

Based on study by Inam (2009), the addition of 1 wt % CNT in the Al_2O_3 nanocomposite were increased the fracture toughness by 103% and flexural strength by 20% higher compared to unreinforced alumina ceramics. Figure 2.13 shows the SEM micrographs of the nanostructured Al_2O_3–TiO_2 composite powders. This show the effect milling processing on nanostructured spherical composite powders with particle size ranged from 50µm and 500nm.

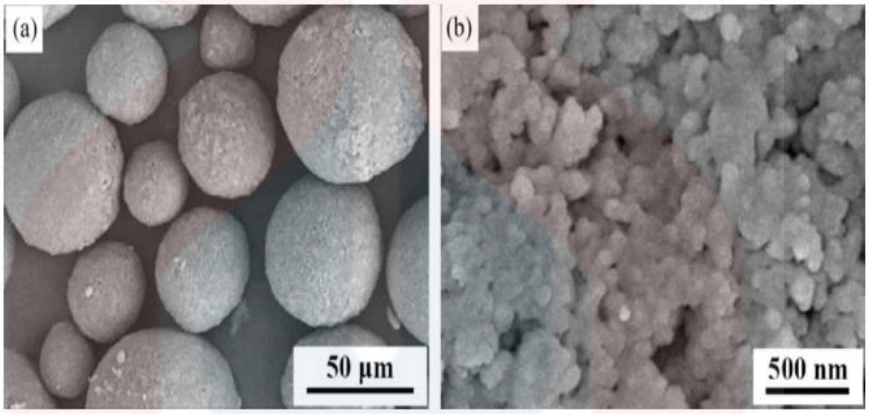

Figure 2.13: SEM micrographs of the nanostructured Al_2O_3–TiO_2 composite powders with different magnification (Bian et al., 2012)

CHAPTER 3

MATERIAL AND METHOD

3.1 Introduction

The material and experimental work did in this study were explained detail in this chapter. $Al_2O_3 - TiO_2 - CNT$ composite were prepared according different parameter of milling time and compaction pressure. The experimental work of producing the Al_2O_3–TiO_2–CNT composite by powder metallurgy (PM) method will be conducted through milling and compaction of $Al_2O_3 - TiO_2 - CNT$ that were discussed. Then, Al_2O_3–TiO_2–CNT were characterized by using several methods to evaluate the effect of different milling time and compaction pressure.

3.2 Raw Materials

The material used in this experiment were Al_2O_3 (> 99.9% purity, average particle size > 20 µm), TiO_2 (> 99.5% purity, average particle size > 21 nm) and CNT (99.9% purity, average particle size > 20 µm). The composition was used in this study to prepare $Al_2O_3 - TiO_2 - CNT$ composite and has been purchased from Sigma Aldrich Company.

3.3 Powder Mixture

The compositions of Al_2O_3−TiO_2−CNT powders were calculated regarding to weight percentages (wt.%) using rule of mixture as presented in Table 3.1. Using method of proportion, the mass of Al_2O_3, TiO_2 and CNT for the powder mixture is can be calculated as 14, 5.6 and 0.4 g, respectively. Before milling process N-heptane was added which is 2% to powder of mixture Al_2O_3−TiO_2−CNT powder mixture as control agent. N-heptane added to reduce die wall friction and agglomeration during compaction (Fathy et al., 2015).

Table 3.1: The composition of Al_2O_3-TiO_2-CNT

Material	Composition (wt %)
Al_2O_3	70
TiO_2	28
CNT	2

The Al_2O_3−TiO_2−CNT powder mixtures are mixed in low energy ball milling with different milling time (15, 30, 45 and 60 h). Figure 3.1 demonstrates the image of custom made low energy ball milling machine. In order to increase the efficiency of milling process, the alumina ball 10:1 to powder ratio with size 10 mm were used and kept constant through this experiment for all parameters of milling time. The rotational speed for ball milling reminded at 200 rpm. The detailed process of milling of powder mixture was illustrated in Figure 3.2.

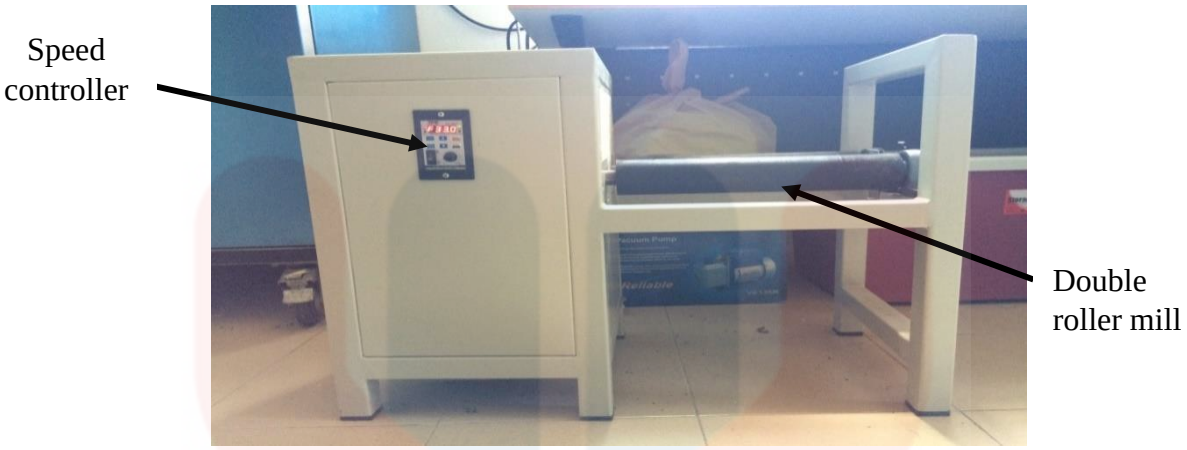

Figure 3.1: Low energy ball milling

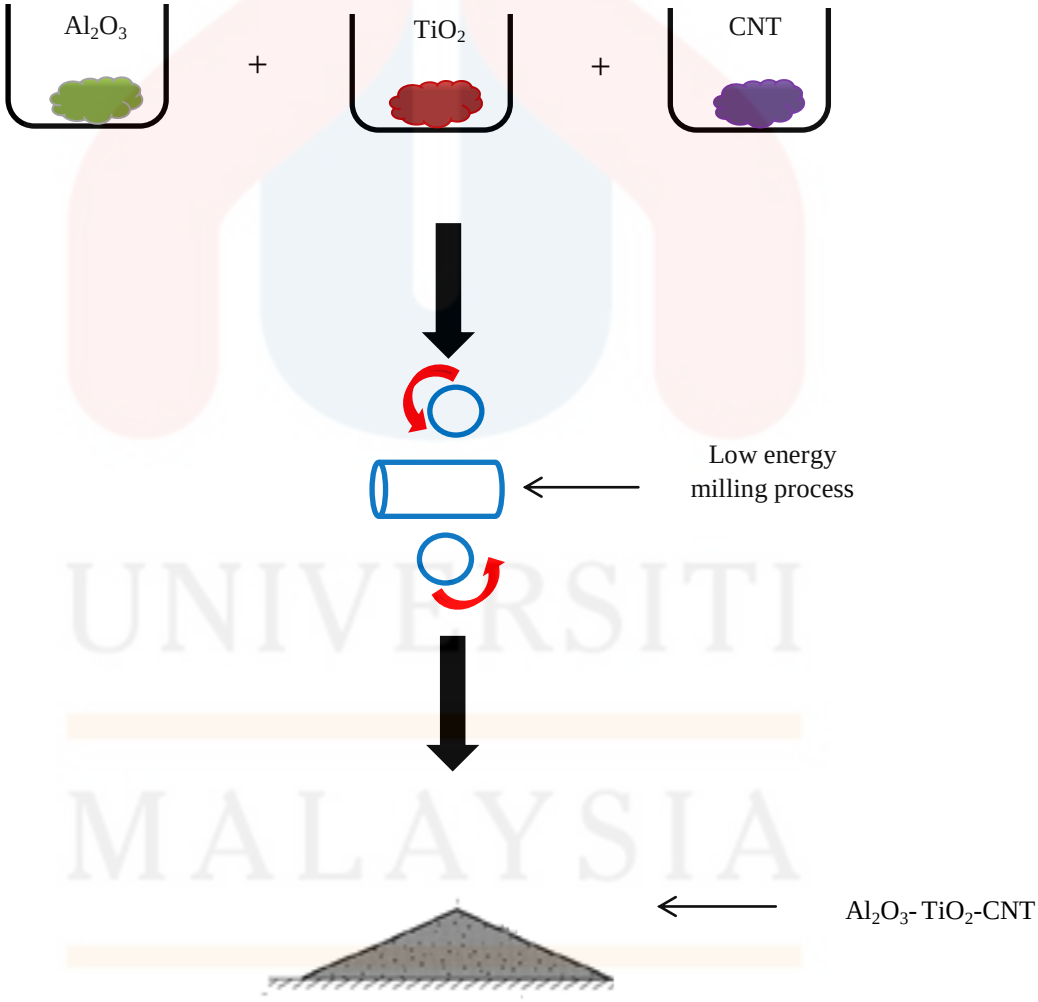

Figure 3.2: Schematic diagram of milling process

3.4 Powder Compaction

In this study, $Al_2O_3-TiO_2-CNT$ were compacted using cold die compaction method to consolidate the powder into bulk form. The $Al_2O_3-TiO_2-CNT$ was compacted in uniaxial single action manual hydraulic uniaxial hand press using stainless steel die with diameter 10 mm at room temperature. The image of stainless steel die shown in Figure 3.3. The die was designed with permit ejection the plunger since applied pressure in unidirectional.

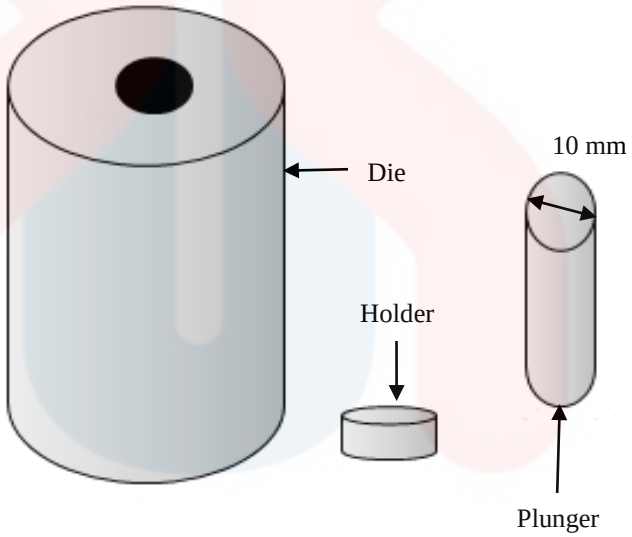

Figure 3.3: Stainless steel die

Prior to compaction, the die mold was cleaned with lubricant oil to reduce friction acting along the die wall and increase the densification compressibility of composite powder during compaction. Moreover, to examine the effect of compaction pressure of composite, the powder mixtures will be compacted at varied pressure with are 200, 400, 600 and 800 MPa (1.6, 3.2, 4.8 and 6.4 tons).

Then, the compacted powder retains for two minutes to avoid from agglomeration and cracked of fine powder before removed from die. Figure 3.4 was despites the detailed process of compaction of powder. To avoid from waste the powder mixtures during compaction in die, the powder need to weight in range between 1.0 to 1.5 g for each pellet of composite.

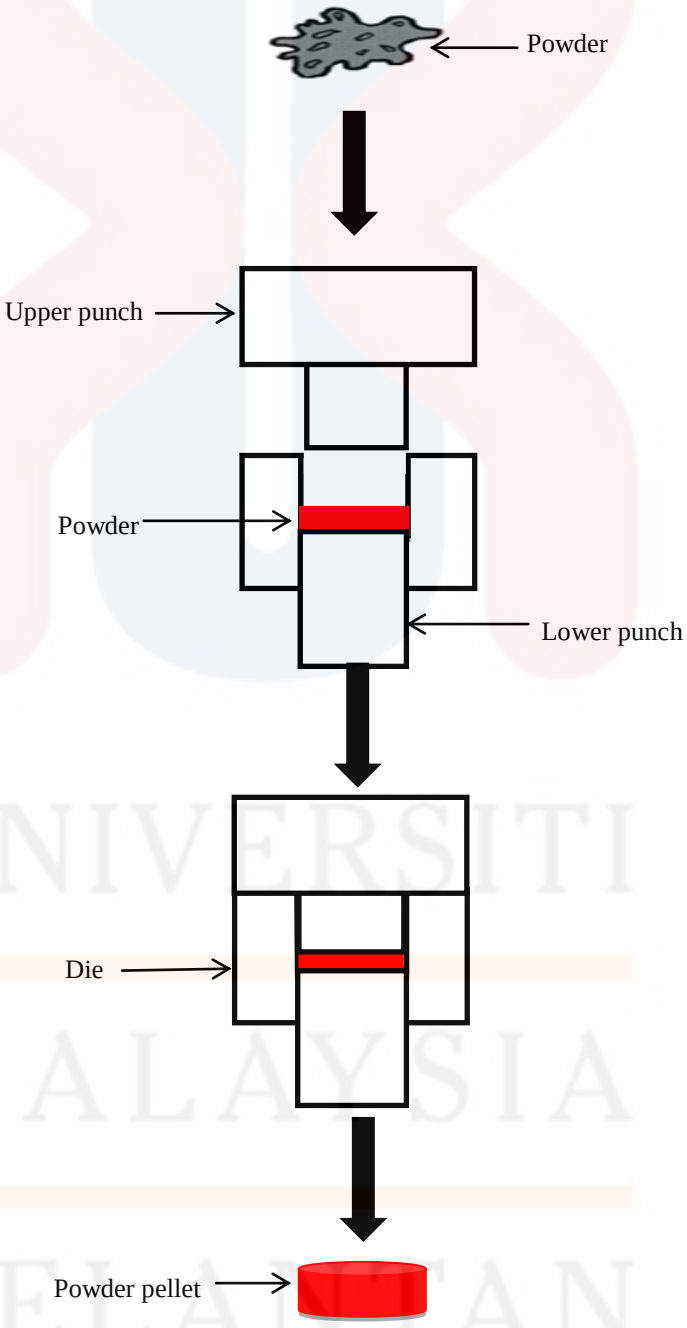

Figure 3.4: Compaction process of powder

3.5 Characterization of Al_2O_3–TiO_2–CNT Composite

The characterization of Al_2O_3–TiO_2–CNT composite will be determined using X-ray diffraction (XRD) analyzer, optical microscope (OM) and green density of composite.

3.5.1 Phase Analysis

XRD analyser (D2 phases, Bruker) was used to characterize the phase identification of raw material of each sample for Al_2O_3,TiO_2 and CNT before mixed. Then, $Al_2O_3 - TiO_2 - CNT$ after milled also observed using XRD analyser to characterize pattern of sample at different milling time. The Cu Ka radiation (λ = 0.154 mm) was used in the scan range of 20^o to 90^o of 2θ angle with step size of 0.02^o. The Software DIFFRAC. EVA phase identification of X-Ray diffraction pattern was used to perform qualitative and quantities analysis of the Al_2O_3–TiO_2–CNT composite. The qualitative information was used to determine the crystallite size, internal strain, dislocation density and lattice parameter and others.

Full width at half maximum (FWHM) as determined by X Ray diffraction was used to calculate and compared the grain size of powder specimens before mixed and after mixed at different milling time (15, 30, 45 and 60 hours). Williamson-Hall method (WH) is method used to evaluate the crystallite size and internal strain after powder was compacted. WH was used and FWHM from Diffrac. EVA was used to identify Al_2O_3 crystallite size and internal strain (Mahani, 2012).

A main criterion to assess the WH method is elimination of contributing peak broadening by instrument. The reference sample was Al_2O_3 which has been compacted at 200, 400, 600 and 800 MPa. Bo and Bi are FWHM (in radians) for

experimental and reference sample, respectively and were obtained from Diffrac. EVA. Only two Al_2O_3 peaks of $(\bar{1}\ 1\ \bar{2})$ and $(\bar{1}\,14)$ reflections were considered for calculating Al_2O_3 crystallite size and internal strain since the other peak are seen overlapped with others peak after milling. Bi of Al_2O_3 pellet was determined as 0.1 g. The slope of plot of Br cos θ against sin either in positive or negative sides indicates θ connection whether the sample in stress or stress-free state.

$$B_o = B_i - B_{crys} + B_{strain} \quad \text{(Eq.1)}$$

Where B_i broadening due to instrumental, B_{cryst} broadening due to size and Bs_{train} broadening due to strain. Subtracting the instrumental effect, Eq. 2 (Mahani, 2012) becomes:

$$B_r = B_{crys} + B_{strain} \quad \text{(Eq.2)}$$

In this case Br represents the overall broadening after eliminating the instrument broadening. Therefore, due to crystallite size and internal strain, WH method is given by (Zuhailawati & Mahani, 2009):

$$B_r \cos\theta = \frac{k\lambda}{D} + \eta \sin\theta \quad \text{(Eq. 3)}$$

Since the $(\bar{1}\,1\bar{2})$ and $(\bar{1}\,14)$ reflections were derived from the same crystallite therefore, a straight line was drawn, according to the data points

3.5.2 Morpology

To investigate the changes of powder before and after milled, the powder was evaluated using optical microscope (OM), Jenoptik Progres CT3, MEIJI TECHNO, Japan with metallurgical series. Evaluation of microstructure of sample was conduct to observe the changes of paticle size of powder and the shape microstructural of different material was formed. Before characterize the microstructure, powder was crushed used the mortar, to reduce the agglomeration of sample during observed under OM. Observation microstructure of powder was characterized at different magnification (5x, 10x and 20x) to get accurate image microstructure of sample.

3.5.3 Green Density

The dimension and mass of composite was measured after compaction. Then, green density (GD) of the composites were calculated using general theory equation (equation 4) after measure the dimension and mass of composite pellet compation. In order to determine the GD of composite:

$$GD = \frac{m}{V} \qquad \text{(Eq. 4)}$$

where:

m = mass

V = volume

In order to study the compressibility of produced composite, densification parameter should be calculated. Densification parameter was determined using Equation 5

$$\text{Density} = \frac{\text{GD}-\text{AD}}{\text{TD}-\text{AD}} \quad \text{(Eq. 5)}$$

where,

GD = Green density

AD = Apparent density

TD = Theoritical density

3.6 Research Flowchart of Al_2O_3–TiO_2–CNT Composite Preparation

The overall of experimental process for $Al_2O_3 - TiO_2 - CNT$ composite preparation was demonstrated in Figure 3.5.

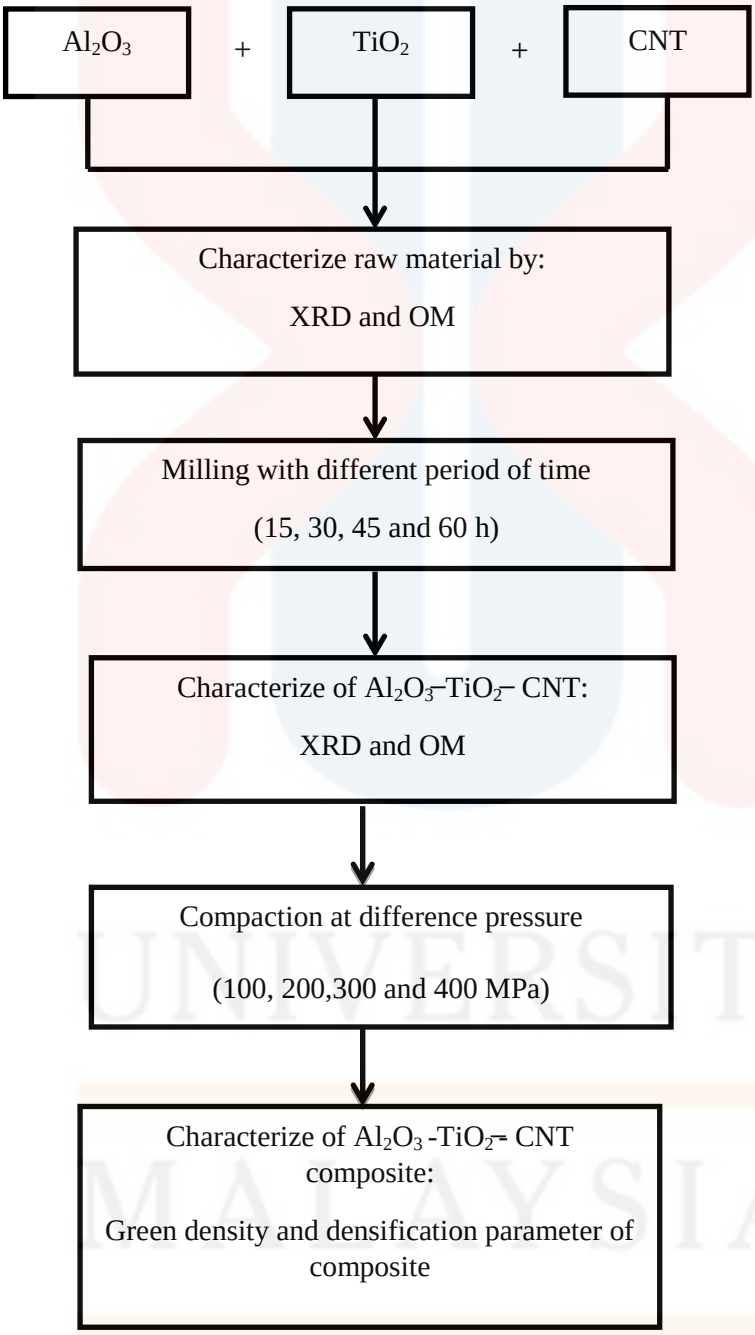

Figure 3.5: Experimental process for Al_2O_3-TiO_2 –CNT composite preparation and characterization

CHAPTER 4

RESULTS AND DISCUSSION

4.1 Introduction

This chapter explained the result obtains from the experimental work in Chapter 3 for characterization of alumina-titania-carbon nanotube ($Al_2O_3 - TiO_2 -$ CNT) composite prepared by powder metallurgy method. In this sections also were described about the effect of milling time and compaction pressure due to structural and microstructure properties of composite.

4.2 Effect of Milling Time

The experiment performed to evaluate the effect of milling parameter on $Al_2O_3 - TiO_2 -$CNT composite. The powder mixture was milled with several milling times, as well as the use ball size 10 mm. N-heptane was also added reduce agglomeration powder mixture during milling. The characterization of XRD patterns was done to study the effect of milling time to the powder mixture.

4.2.1 XRD Pattern of Pure Powder

The characteristic pure powders were analysed using XRD. Figure 4.1 shows the XRD pattern of Al_2O_3, TiO_2 and CNT. Based on XRD result, the pure powders were analysed to have crystalline structure. The Al_2O_3 powder was observed that have four strong peaks at 25.62˚, 35.21˚, 43.43˚ and 57.61˚. While, the analysis shows

the TiO_2 powder also have three sharp peaks at 25.31˚, 36.92˚ and 48.04˚. However, the other peak appeared show no strong because of short and broadening.

The Al_2O_3 revealed as corundum phase while TiO_2 showed well defined diffraction peaks corresponding to anatase phase, that form stable rather than rutile and brookite. This similar with the previous research by Bian et al. (2012); Rocha et al. (2013); Sivakumar et al. (2004) that was discussed in Section (2.8.1). Thus, the finding in Figure 4.1 shows the same peak presented of pure powder of Al_2O_3 and TiO_2 as well as described in Figure 2.9.

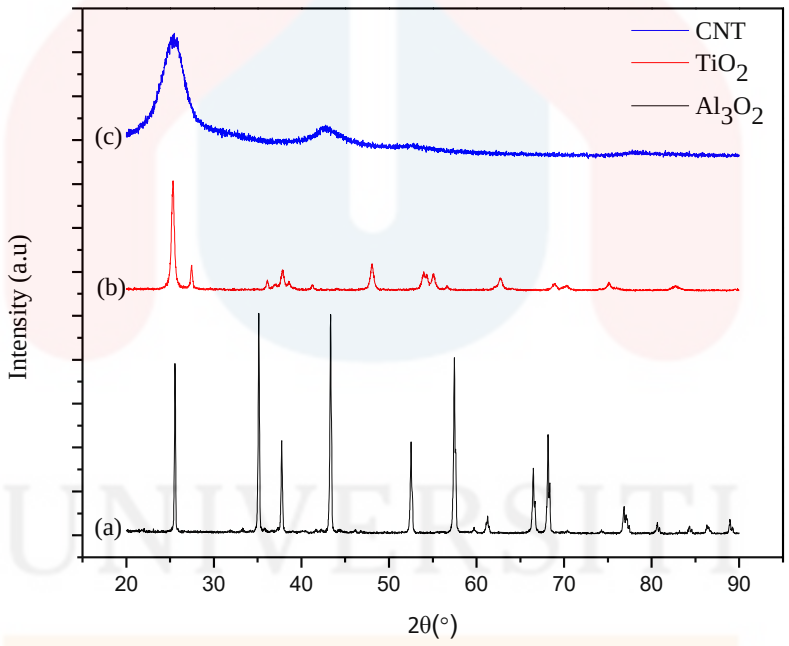

Figure 4.1: XRD patterns of (a) Al_2O_3 (b) TiO_2 and (c) CNT powder

For both of Al_2O_3 and TiO_2 peak exhibit the strongest peak are at 35.03˚ and 35.15˚ that also present same to previous study that revealed in Figure 2.10. In Figure 4.1 the crystalline peak of CNT powder, highest intensity is obtained at position 24.66˚ and short peak at 44.67. Both crystalline peak of CNT powder was show not

strong peak, this is due to high solid solubility of CNT and peak found in amorphous structure (Mahani, 2012; Yavas et al., 2015).

4.2.2 XRD Pattern of Milled Powder

Figure 4.2 showed the result of XRD pattern of Al_2O_3-TiO_2 –CNT powder mixture at different milling time (15, 30, 45 and 60 h) with 10 mm alumina ball. Al_2O_3 and TiO_2 phases are observed having crystalline structure while CNT phase has very weak peak obtained after milled. The crystalline phases were obtained with different milling time provide no sign of amorphous phases have seen in diffraction peak for all milling time. The first crystalline peak of Al_2O_3, TiO_2 and CNT indicate was overlapped each other, due to their peak are seen much closed at 15 and 30 h of milling time. The peak crystallite structure of Al_2O_3 was seen at 25.57˚ for both 15 h and 30 h. The peak TiO_2 phase was presented at 25.30˚ for 15 h and small shifted to the left at 25.48˚ and no difference of 2θ for CNT peak at 25.63˚ for both 15 h and 30 h.

Based on figure, the four strong peaks of Al_2O_3 has appeared at hkl $(\bar{1}0\bar{1})$, $(\bar{1}\,14)$, $(\bar{2}\,1\,\bar{3})$, and $(\bar{2}\,1\,\bar{6})$ become shorten and diminished with increasing milling time. Besides that, the peak of Al_2O_3 also reduce size of particle and become more wider according to the grain size become refining with increasing of milling time (Hussain and Yusoff, 2011; Liu et al., 2014).Peak of TiO_2 also appeared at hkl $(\bar{1}\,0\,1)$, $(0\,0\,\bar{4})$, and $(\bar{1}\,0\,\bar{5})$ and slightly diminished due to small size with increasing the milling time.

Apart from that, TiO_2 phase was easy to diffuse into matrix phase of Al_2O_3. CNT has shortened peak and not observed at all milling times, presumably as a result of its faster diffusion into the Al_2O_3 matrix than TiO_2. That is, solid solubility for CNT in Al_2O_3 is far higher than that of TiO_2, and can be later diffused into a solid Al_2O_3 solution. Moreover, the evidence of formation of Al_2O_3 solution can be described by shifted Al_2O_3 peaks to the left with prolonged milling time.

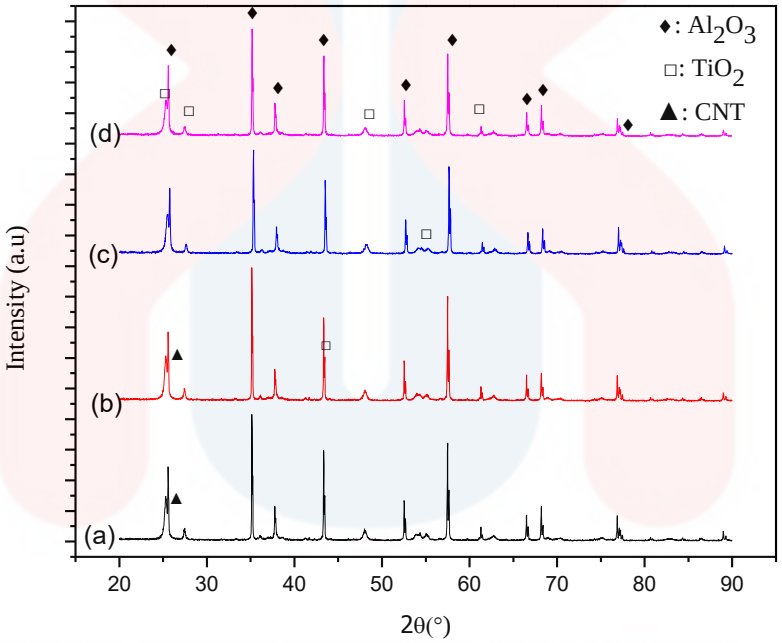

Figure 4.2: XRD patterns of milled powder at (a) 15 (b) 30 (c) 45 and (d) 60 h

Brittle phase powder basically dissolves into ductile matrix phase during milling. Two methods was used to describe the solubility of powder, there are peak disappearance and peak shift. In this experiment, the methods were used to discuss the solubility of Al_2O_3, TiO_2, and CNT in Al_2O_3 again milling time. The formation of second element into matrix phase of Al_2O_3 was discovered by peak disappearance in XRD pattern. The peak shifts either to the right or left of 2θ angle axis is also another method to determine dissolution of second phase into matrix lattice.

In this experiment, no visible peak shifting is observed at early milling time. This due to low energy ball milling was used at only 200 rpm and shorten milling time that not enough to form new phase of solution. This can explain by limitation amount of Al_2O_3 solution that not contributes to the change of Al_2O_3 lattice. There was no transformation of TiO_2 and CNT into Al_2O_3 phase during the milling process. Based on figure above, its can discovered that peaks of Al_2O_3 and TiO_2 are show broadened.

Besides, the wider peak occurs due to internal stress accumulation induced by formation and the presence of tiny particle of second phase that introduce defect. The crystallite size and internal strain of powder mill not easy to change by milling time 15, 30, 45 and 60 h due to little shift peak to left was formed. Based on result, the 60 h of milling time provide strong formation of second phase of Al_2O_3-TiO_2 –CNT powder.

4.2.3 Crystallite size and internal strain of milled powder

In order to deform the crystallite size and internal strain of milled powder, the WH method was doned used. First, linear regression of $B_r cos\theta$ data points where it explains the strain is involved whereas if these values are constant, the formation of broadening refer to effect of size powder. According to Yang et al. (2009) negative intercept is attributes to the differences in penetration depth with the increase of 2θ angle. The chosen of low 2θ angle of peak width refer to negative result of intercept in the WH plot was get and it become indicates possible broadening due to size.

Figure 4.3 demonstrates the WH plots of $B_r\cos\theta$ againt $\sin\theta$ for Al_2O_3 different milling time of 15, 30, 45 and 60 h. A straight line was drawn to the corresponding data at hkl $(\bar{1}\,1\,\bar{2})$ and $(\bar{1}\,14)$,. Based on Figure 4.3, does not have negative intercept and slope present with increasing milling time, it indicate that the crystallite size was descreased with increasing internal strain.

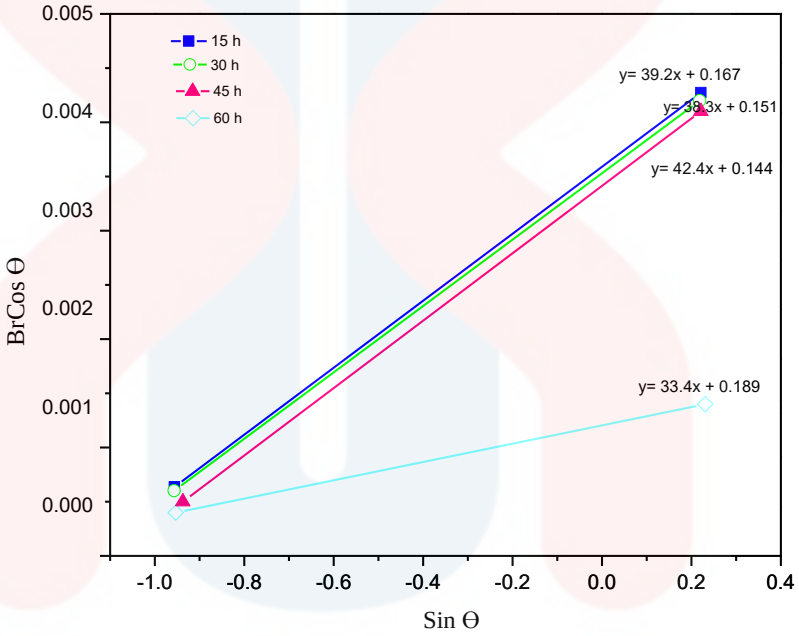

Figure 4.3: Plot of Brcos θ against sin θ for calculating crystallite size and internal strain for the powder milled

Figure 4.4 present the value of Al_2O_3 crystallite size as a function of milling time for milled the powder with 10 mm alumina ball. Before milled, Al_2O_3 powder particle have a crystallite size in nanometer range because Al_2O_3 already has fines sizes. Al_2O_3 crystallite size was defined by FWHM that taking from hkl peaks at $(\bar{1}\,1\,\bar{2})$ and $(\bar{1}\,14)$. Al_2O_3 crystallite size slightly reduced to 0.9 nm with increasing milling time to 30 h from 39.2 nm. However, the crystallite size of Al_2O_3 increase to 42.4 nm at 45 h of milling time while decreasing again to 33.4 nm with increasing

milling time to 60 h. This show that the particle size of Al_2O_3 powder during milling not fully homogenous and agglomerate between each other with TiO_2 and CNT, that caused the grain fining of Al_2O_3 at 45 h not really well compare to 60 h. It slightly inversely proportional different with the previous research by Sivakumar et al. (2004) that the Al_2O_3 crystallite size decrease with increasing milling time.

Addition, in milling time should reduce Al_2O_3 crystallite size since repeated deformation occurs at a higher rate over time. Apart from that, when energy supplied to powder increase each crystallite remains constrained by its surrounding crystallites and produced stress over strain in the composite. Besides, decreasing crystallite size also occurs due to the introduction of defects such as dislocations within a grain during the milling process.

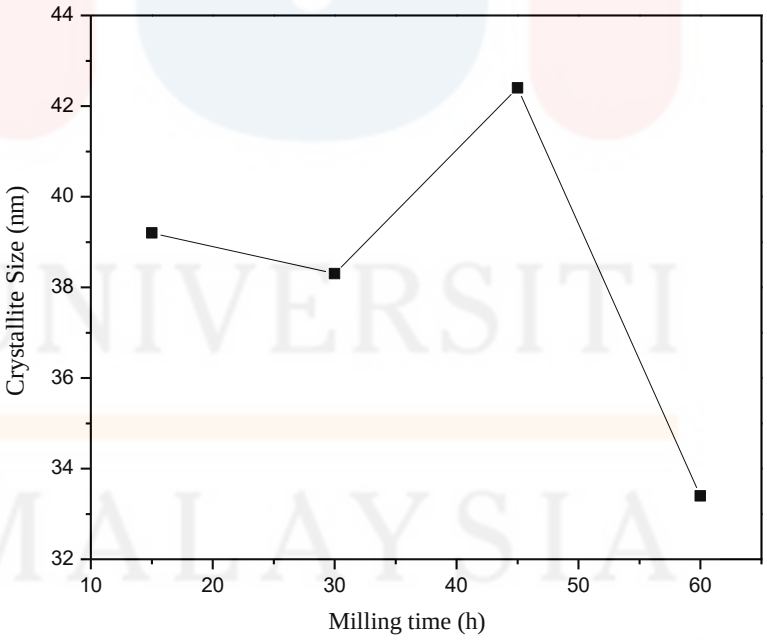

Figure 4.4: Al_2O_3 crystallite size of milled powder with different milling times

The internal starin of Al_2O_3 powder against milling time was shown if Figure 4.5. The internal strain of Al_2O_3 milling is marginally increase as increasing the milling time, due to stress relieving accompanied with annihilation of dislocations during milling. Strain was divided into uniform strain and non-uniform strain. This refer to changing of peak broadening of peak shift of atom that cause unit of cell increase or decrease according to crystallite size of Al_2O_3. The internal strain of Al_2O_3 powder was proposed by WH method due to sharp peak width of broadening.

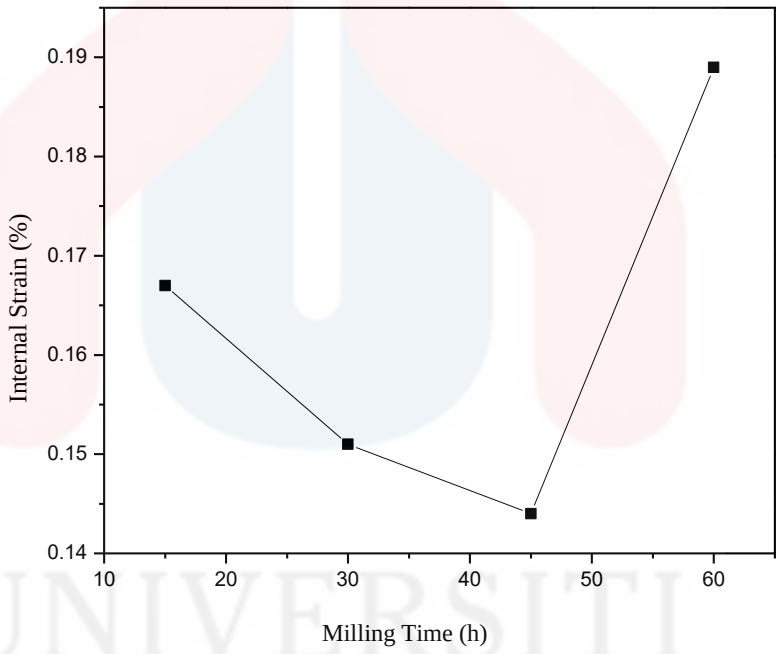

Figure 4.5: Al_2O_3 internal size of milled powder with different milling times

Based on figure above, the percentage of internal strain of Al_2O_3 decreased to 0.016 % from 15 h to 30 h of milling time. The rapidly decreasing of internal strain also occurred at 45 h with 0.144 % of internal strain. The internal strain should be increase with reducing the crystallite size. However the internal strain of Al_2O_3 powder increase rapidly to 0.189 % when powder mixture milling at the 60 h.

This result indicates that internal refinement occurs when the milling time increase collision occurred between the powder and ball mill at 60 h was optimized. This also occurred due to formation of strain hardening of powders during milling process. Figure 4.6 demonstrates the Al_2O_3 crystallite size and internal strain of as-milled powder with different milling time. Thus, this obviously shows the Al_2O_3 crystallite size is observed to vary inversely to internal strain for all milling times. Although only the Al_2O_3 crystallite sizes at 45 h increase while the internal strain decrease.

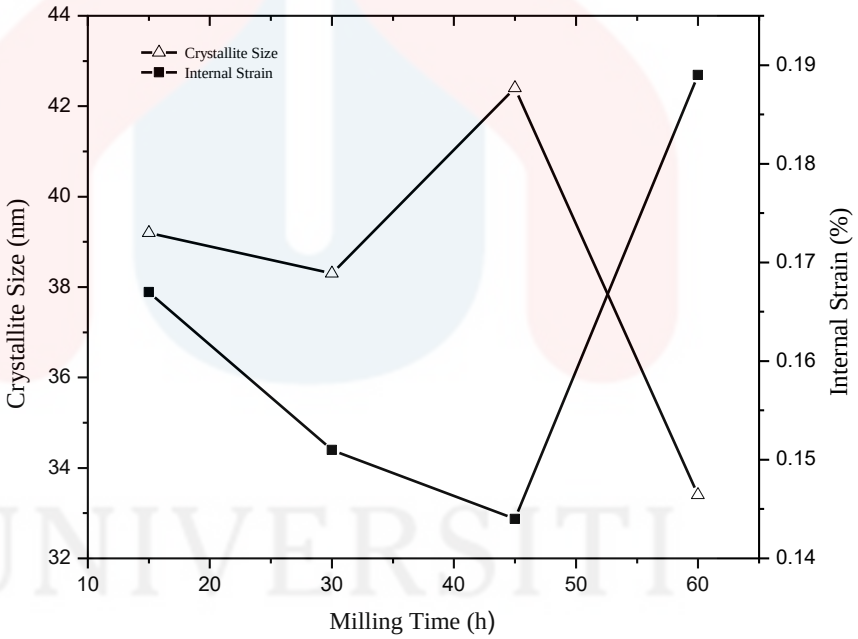

Figure 4.6: Al_2O_3 crystallite size and internal strain of as-milled powder with different milling time

4.2.4 Microstructure Characterization of Pure and Milling Powder

Figure 4.7 shows the optical microstructure images pure powder of Al_2O_3, TiO_2 and CNT. The three different particles that revealed in the figure were obtained. In Figure 4.7 (a) represents the image of grey particle microstructure with rich side of Al_2O_3. The particle size of TiO_2 powders is smaller rather than Al_2O_3 and CNT powder. This due to the size of starting powder TiO_2 in nanometer (nm) size in average size 20 nm compare to Al_2O_3 and CNT are in micrometer (μm) size with average size 20 μm. The black small hollow particle was deformed in with Figure 4.7 (c) was captured as CNT powder. As comparison, the irregular shape and different particle size due to all pure powder microstructure.

In Figure 4.8 presents the image optical microscope for milled powder mixture at various milling time for the powder milled with 10 mm alumina ball at 20x magnifications. The microstructure consists of uniformly particle distributed in all milling period and containing some changes in particle size and shape. As can be seen in these figures, is that with increment of the milling, the powder mixture tends to densify, because there is decreasing in the particle size and number of pores in there. The increasing the milling time will reduce the porosity of powder due to small powder of TiO_2 and CNT was diffused onto bigger size of Al_2O_3 matrix and fill the void. This situation confirms the results of the green density measurements that will discuss below.

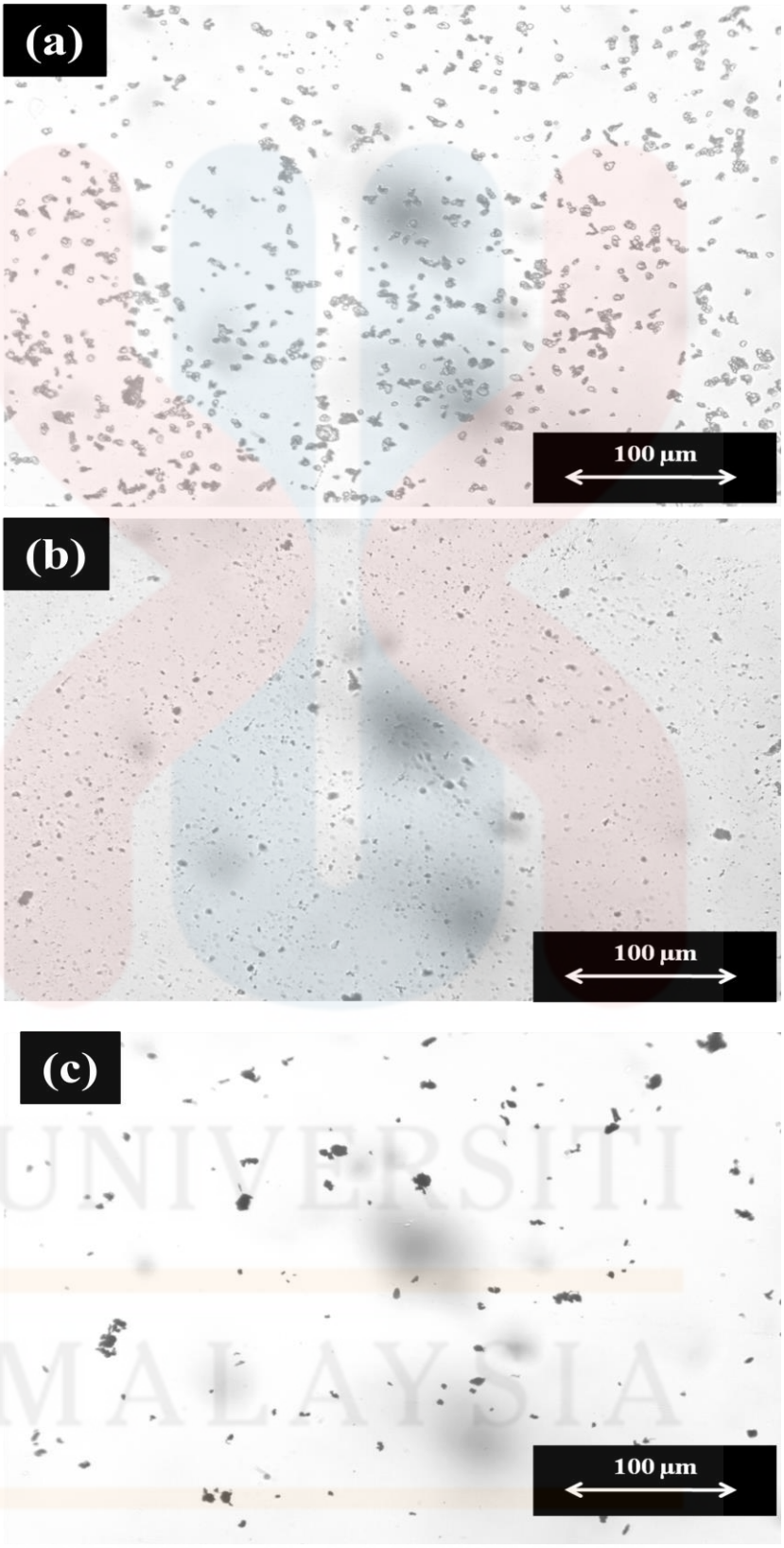

Figure 4.7: Optical microscope images of pure power (a) Al_2O_3 (b) TiO_2 and (c) CNT

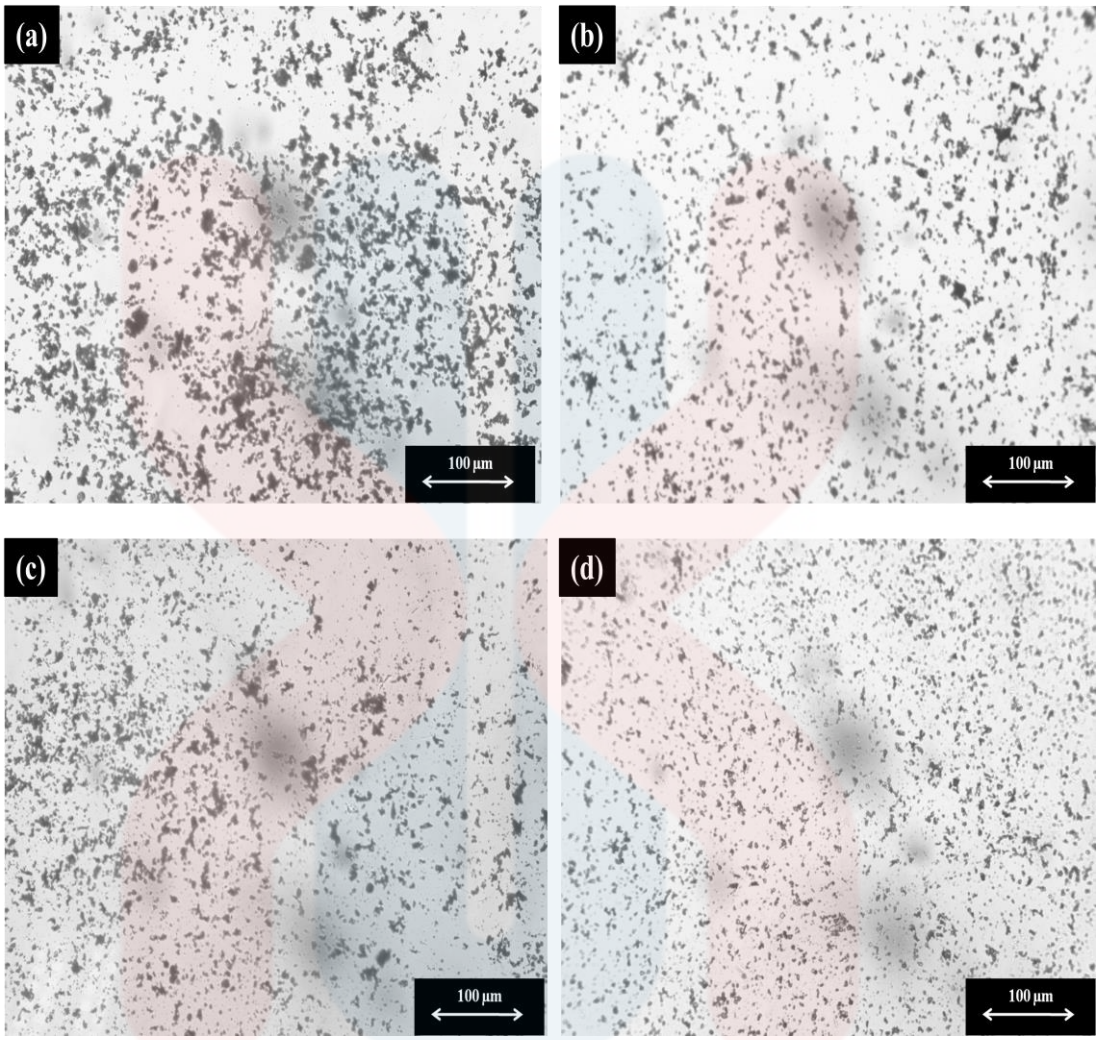

Figure 4.8: Optical microscope images of milled power (a) 15 (b) 30 and (c) 45 and 60 h

The increase in homogenous particle size and finer grain size can be seen at 60 h compare to the particle size distribution forming at 15 h of milling time. This due to not enough energy provides to break the particle of Al_2O_3 matrix during 15 h of milling time. Another important observation that can described according to increasing milling time from 15, 30, 45 to 60 h, they have show in homogeneous particle microstructures was produce and reduction in Al_2O_3 matrix grains size (Xiao et al., 2011; Yavas et al., 2015a) was provided based on figure below.

Furthermore, powder particles are trapped between balls due to ball to ball collision during milling proecess. In this condition, the fracture break of powder mixture composite particle was deform with prolonged the milling time. In overall, the particle size and shape of powder mixture become finer and small void that can increase the fracture toughness and ductility of $Al_2O_3-TiO_2-CNT$ composite. However, the image of optical microscope cannot give high quality image due to lack of magnification.

4.3 Effect Compaction Pressure

The compaction using hand pressing was done in this work, in order to increase the density of powder mixture. The effect of compaction pressure was related according to different milling time. This contributes to reduce the porosity of powder that basically cause the sample brittle due to low density of powder. Different compaction pressure was allowed to formation of compaction powder with 200, 400, 600 and 800 MPa using 10mm size of die. This subtopic was discussed detailed about green density and densification parameter of $Al_2O_3-TiO_2-CNT$ composite.

4.3.1 Green Density of Different Milled Time

Green densities (GD) of $Al_2O_3-TiO_2-CNT$ powder compact are plotted against milling time and compaction pressure shown in Figure 4.9. As been seen in figure below, the milling powders were found increase in GD with increasing the compaction pressure. At pressure 200 MPa, the powder mixture at 15 h has higher GD compare to 30, 45 and powder milling at 60 h present lowest GD. The result GD

at 400 MPa of compaction pressure present that powder mixture at 45 h of milling time has highest GD value which is 2.76 gcm^{-3} , while the lowest GD at this pressure reach to 60 h of milling. Both 600 and 800 MPa of compaction pressure produce same of type of GD deform. It indicates the GD has highest value at 45 h and tends decreasing according to 30, 60, and 15 h. According to result that represents in figure below, the increasing of milling time not promising to provide high value of GD.

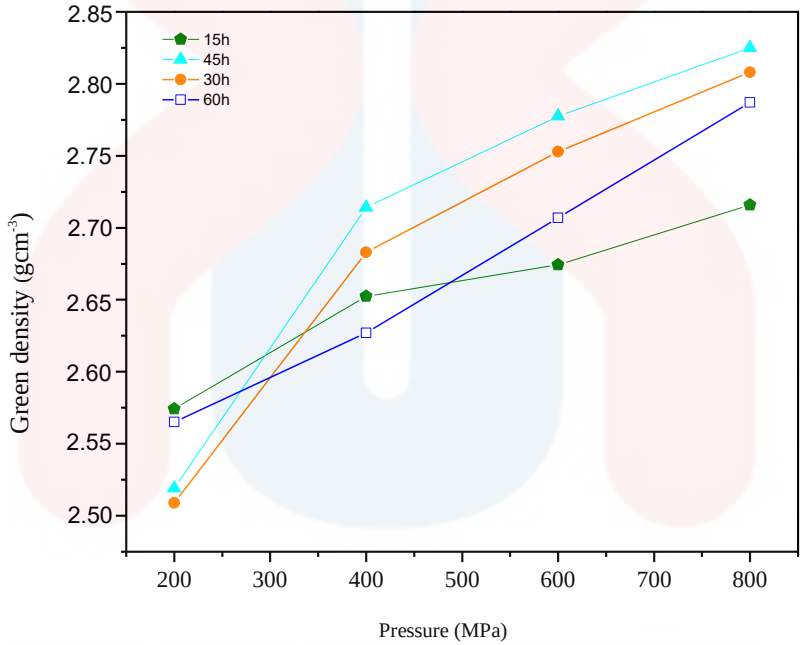

Figure 4.9: Green density (GD) of powder compact with different milling times and compaction pressure

The factor that contributes to increase in GD was described as microstructure, particle size of powder and formation of ductile powder mixture during compaction. The ductility of sample will revealed during compaction. In this experiment the compaction of powder difficult to form according to pressure applied during compact. Moreover, Mahani, (2012); Qiu et al. (2015) discussed that the finer and small particle of powder that provided by extended milling time will increase the GD

and it seem that it have better particle packing during compaction and leading to produce dense composite. High pressure indicates to decreasing of volume porosity Hackemann et al. (2010), it provided to powder of TiO_2 and CNT fill the void of its Al_2O_3 matrix. Thus, the powder mixture of Al_2O_3−TiO_2−CNT composite has highest GD at 45 h of milling time compare to other powder mixture.

4.3.2 Densification Parameter of Milled Powder

In order to discuss the effect of compaction pressure on the composite, the graph densification parameter (DP) against pressure was plotted in Figure 4.10. Increasing on compaction pressure provide good DP of the composite body. In this experiment the highest DP was provided by powder mixture that milled at 45 h while powder mixture that milled at 15 h has lowest DP. It can be observed that the better pressure is between 600 to 800 MPa. This due to the variations of compaction pressure that applied can contribute to produce good powder packing. Besides, particle fragmentation becomes easier because deformation has been enhanced, leading to an increase in composite density. Under much higher compaction pressure, the composite experience high plastic deformation that continuously increased DP.

According to result provided below, the smaller particle size that produce during milling process which has broad distribution has higher possibilities to fill in the space between the coarser one, it therefore exhibited higher particle packing.The compact which was pressed by high pressure had less porosity owing to it having higher number of point contact and contact area. The compaction pressure Al_2O_3− TiO_2 − CNT composite difficult to applied due to ductile properties of powder.

Therefore, fracture toughness of powder was increased because it can be enhanced when composite has high densification.

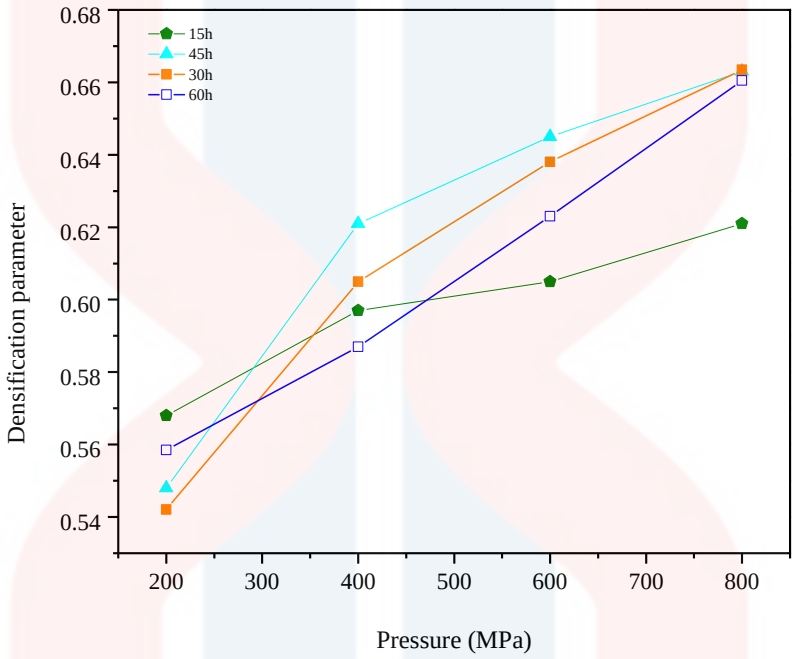

Figure 4.10: Densification parameter powder compact with different milling time as a function of compaction pressure

During compaction, plastic deformation of powder mixture can be formed. The pressure applied to contact area between the grains increases that tendency to particle powder become plastic deformation. Compressibility is a measure to which a powder will compress or densify upon application of external pressure. To relate between density with plastic deformation, the Panelli and Ambrosio Filho equation was analyzed (Katheria & Singh, 2015).

$$\ln\left[\frac{1}{1-D}\right] = AP^{\frac{1}{2}} + B \qquad \text{Eq 4.1}$$

where,

D= relative density of the compacted material (gm/cm3)

P= applied pressure or Compaction pressure (MPa)

A= plastic deformation or deformation capacity of the powder during compaction process.

B= fitting constant

The parameter A, inclination or slope from the linear plot, provides the plastic deformation capacity of the powder in compaction. Thus as the parameter A increases the powder will undergo more plastic deformation during compaction. Figure 4.10 show the compresiblity of curve of powder mixture with differnet milling time. The powder mixtrure at 45 h show the higher curve, this show pastic deformation of powder mixture 45 h of milling time has highest plastic deformation, it can enhance by high density of powder.

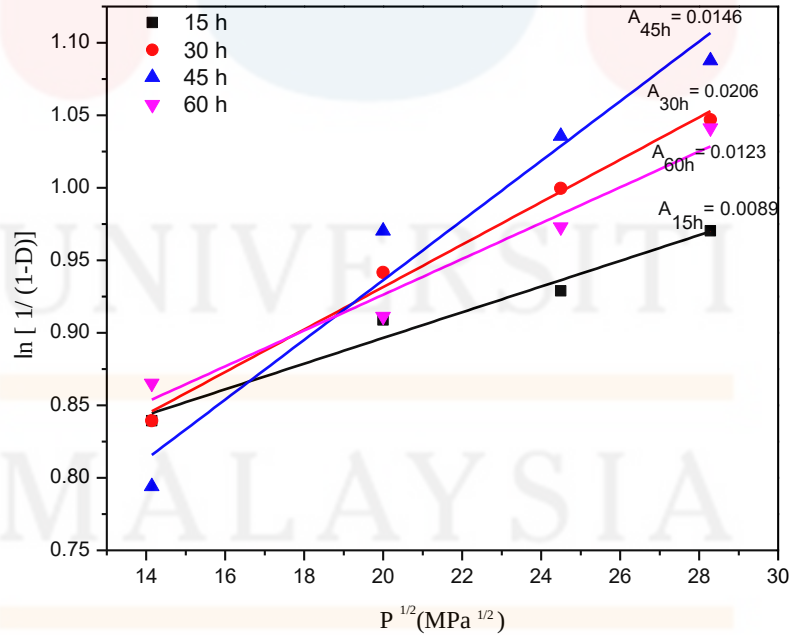

Figure 4.11: Plot of experimental data for green compact using the equation proposed by Panelli and Ambrozio Filho

CHAPTER 5

CONCLUSION AND RECOMMENDATION

5.1 Conclusion

In this experiment, the characterization of alumina titania carbon nanotube composite prepared by powder metallurgy method was already done. The powder mixture was prepared by using low energy milling with variation on time at 15, 30, 45 and 60 h. The compaction pressure also was prepared at difference pressure with 200, 400, 600 and 800 MPa. Therefore, the conclusion was described according to variation of milling time and compaction pressure. The conclusions were drawn from,the phase indentification, crystallite size, morphology, green density and densification parameter.

i. Based on XRD pattern no visible new phase was formed when increasing milling time.
ii. The lowest crystallite size of and highest internal strain $Al_2O_3-TiO_2-$ CNT are at 60 h.
iii. Different milling time that applied to $Al_2O_3-TiO_2-CNT$ powder was already give effect to microstructure of powder, the coarse particle size and shape become fine and reduction in size according to homogeneous particle microstructures produce when small powder fill the the void of Al_2O_3 matrix.
iv. Milled powder that milling at 45 h provided highest green density and densification parameter of $Al_2O_3–TiO_2–CNT$ composite with increasing the compaction pressure.

Thus, this can conclude that, fracture toughness, plastic deformation and ductility of powder increasing with increment the pressure.

5.2 Future Work Suggestions

The milling parameter that used in this experiment show only minimizes changed form to microstructure and structural composite. The low energy ball milling machine show few changes on phase of powder. Therefore, for the future, powder need to milling at high speed energy ball milling to produce enough energy to change the phase.

Besides, milling parameter like different ball size, milling speed also need to applied in order to study the effect of milling parameter on composite powder.The microstructure that capture by optical microstructure not provides well imaged due to limitation in magnification to capture high quality image. Thus, in future, use the field emission scanning electron microscope (FESEM) with EDX to produce high definition image with 3D image according to can capture at high magnification. Apart from that, the transmission electron microscopy (TEM) machine also one of better microscope, in order to produce image of microstructure that very clear.

Moreover, in future, The addition of variation compaction pressure also need to take action, to produce composite that have high density with low porosity, in order to reduce the brittle. Furthermore, $Al_2O_3-TiO_2-CNT$ composite need to sintered at various temperatures to increase the properties of composite and reduce the porosity of powder that can tend to brittle.

Surface analysis also can be further detail in future work. In order to study the surface area of solid material using bruenaur-emmelt teller (BET) machine. The specific surface area of composite can be observed using this machine. So that, the measurement porosity of powder can be observed using BET.

Moreover, in order to go deep study in powder metallurgy field, the Al_2O_3–TiO_2–CNT composite need to process using variation method like hot pressing (HP), hot isostatic pressing (HIP), sol gel (SG) and mechanical alloying (MA). In order to produce composite material that has high quality properties that can use in various applications.

REFERENCES

Abdizadeh, H., Ashuri, M., Moghadam, P. T., Nouribahadory, A., & Baharvandi, H. R. (2011). Improvement in physical and mechanical properties of aluminum/zircon composites fabricated by powder metallurgy method. *Materials and Design*, *32*(8–9), 4417–4423.

Aguilar-martínez, J. A., Pech-canul, M. I., & Leyva-porras, C. (2013). Effect of Co_3O_4 content and compaction pressure on the microstructure and electric properties of SnO_2–Sb_2O_5 – Cr_2O_3 varistor ceramics. *Ceramics International*, *39*(7), 8237–8243.

Al-bahadly, E. A. O. (2013). *The Mechanical Properties Of Natural Ekhlas Aboud Osman Al-Bahadly The Mechanical Properties of Natural Fiber Composites*. Swinburne University of Technology.

An, E., Ghiami, A., & Ipek, R. (2015). Int . Journal of Refractory Metals and Hard Materials Effect of high ratio of reinforcement particle size to matrix powder size and volume fraction on microstructure, densification and tribological properties of SiC p reinforced metal matrix composites, *52*, 183–194.

Banga, H., Singh, V. K., & Choudhary, S. K. (2015). Fabrication and Study of Mechanical Properties of Bamboo Fibre Reinforced Bio-Composites, *6*(1), 84–99.

Bian, H. min, Yang, Y., Wang, Y., & Tian, W. (2012). Preparation of nanostructured alumina-titania composite powders by spray drying, heat treatment and plasma treatment. *Powder Technology*, *219*, 257–263.

Bian, H., Yang, Y., Wang, Y., Tian, W., Jiang, H., Hu, Z., & Yu, W. (2012). Alumina – titania ceramics prepared by microwave sintering and conventional pressure-less sintering. *Journal of Alloys and Compounds*, *525*, 63–67.

Callister, W. D. (2011). *Materials Science* (8th ed.). John Wiley & Sons.

Chen, B., Li, S., Imai, H., Jia, L., Umeda, J., & Takahashi, M. (2015). Carbon nanotube induced microstructural characteristics in powder metallurgy Al matrix composites and their effects on mechanical and conductive properties. *Journal of Alloys and Compounds*, *651*, 608–615.

Chen, C., Liu, J., Liu, P., & Yu, B. (2011). Investigation of Photocatalytic Degradation of Methyl Orange by Using Nano-Sized ZnO Catalysts,

Deborah D.L Chung. (2010). *Composite Material* (Second). New York: Springer.

Dehaghani, M. T., Ahmadian, M., & Fathi, M. (2014). Effect of ball milling on the physical and mechanical properties of the nanostructured Co–Cr–Mo powders. *Advanced Powder Technology*.

Dubourg, L., Lima, R. S., & Moreau, C. (2007). Properties of alumina – titania coatings prepared by laser-assisted air plasma spraying, *201*, 6278–6284.

E. Zapata Solvas , D. Gomez,Garcia, A. D.-R. (2012). Towards physical properties tailoring of carbon nanotubes-reinforced ceramic matrix composites, *32*, 3001–3020.

Erdemir, F., Canakci, A., & Varol, T. (2015). Microstructural characterization and mechanical properties of functionally graded Al_2O_{24} / SiC composites prepared by powder metallurgy techniques. *Transactions of Nonferrous Metals Society of China*, *25*(11), 3569–3577.

Esawi, A. M. K., Morsi, K., Sayed, A., Taher, M., & Lanka, S. (2010). Effect of carbon nanotube (CNT) content on the mechanical properties of CNT-reinforced aluminium composites. *Composites Science and Technology*, *70*(16), 2237–2241.

Fathy, A., El-Kady, O., & Mohammed, M. M. M. (2015). Effect of iron addition on microstructure, mechanical and magnetic properties of Al-matrix composite produced by powder metallurgy route. *Transactions of Nonferrous Metals Society of China (English Edition)*, *25*(1), 46–53.

Flores-garcía, J. C., Pech-canul, M. I., Leal-cruz, A. L., & Rendón-angeles, J. C. (2012). Synthesis of Si_3N_4/Si_2N_2O into silicon particulate porous preforms by hybrid system CVI and direct nitridation, *32*, 175–184.

Furlani, E., Aneggi, E., Leitenburg, C. De, & Maschio, S. (2014). High energy ball milling of titania and titania – ceria powder mixtures. *Powder Technology*, *254*, 591–596.

Garg, P., Park, S. J., & German, R. M. (2007). Effect of die compaction pressure on densification behavior of molybdenum powders. *International Journal of Refractory Metals and Hard Materials*, *25*(1), 16–24.

German, R. M. (1997). *Powder Metallurgy Science* (2nd ed.). The Pennsylvania State University.

Giang Nguyen, V., Thai, H., Huynh Mai, D., Trung Tran, H., Lam Tran, D., & Tuan Vu, M. (2013). Effect of Titanium Dioxide on The Properties of Polyethylene/TiO_2 Nanocomposites. *Composites Part B*, *45*(1), 1192–1198.

Gupta, S. K. (20AD). *A Study on Mechanical Behavior of Bamboo Fiber Based Polymer Composites*. National Institute of Technology Rourkela.

Hackemann, S., Flucht, F., & Braue, W. (2010). Creep investigations of alumina-based all-oxide ceramic matrix composites. *Composites Part A: Applied Science and Manufacturing*, *41*(12), 1768–1776.

He, W., Li, C., Luan, B., Qiu, R., Wang, K., Li, Z., & Liu, Q. (2015). Deformation behaviors and processing maps of CNTs / Al alloy composite fabricated by flake powder metallurgy. *Transactions of Nonferrous Metals Society of China*, *25*(11), 3578–3584.

Hideshi Miura. (2014). Advanced Powders Processing , (82).

Hu, C., Li, F., Qu, D., Wang, Q., Xie, R., Zhang, H., … Zhou, Y. (2014). Developments in hot pressing (HP) and hot isostatic pressing (HIP) of ceramic matrix composites. *Advances in Ceramic Matrix Composites*, 164–189.

Huang, J.-L., & Nayak, P. K. (2014). *Strengthening alumina ceramic matrix nanocomposites using spark plasma sintering*. *Advances in Ceramic Matrix Composites*. Woodhead Publishing Limited.

Hussain, Z., Yusoff, M., & Othman, R. (2011). Phase Analysis of Mechanically Alloyed In-situ Copper-Tungsten Carbide Composite, *173*, 67–71.

Inam, F. (2009). *Development of Ceramic – Carbon Nanotube (CNT) Nanocomposites*. Queen Mary, University of London.

Jagannatham, M., Sankaran, S., & Haridoss, P. (2015). Microstructure and mechanical behavior of copper coated multiwall carbon nanotubes reinforced aluminum composites. *Materials Science and Engineering A*, *638*, 197–207.

Kanthavel, K., Sumesh, K. R., & Saravanakumar, P. (2016). Study of tribological properties on $Al/Al_2O_3/MoS_2$ hybrid composite processed by powder metallurgy. *Alexandria Lexandria Engineering Journal*, 3–7.

Katheria, S. K., & Singh, M. K. (2015). To Experimentally Examine the Green Density and Plastic Deformation of the Fe-Gr-Cr Prepared by Compaction Process, *5*(5), 136–140.

Kondoh, K., Threrujirapapong, T., Imai, H., Umeda, J., & Fugetsu, B. (2008). CNTs / TiC Reinforced Titanium Matrix Nanocomposites via Powder Metallurgy and Its Microstructural and Mechanical Properties, *2008*.

Kora, M., Kamberovi, Ž., An, Z., & Filipovi, M. (2006). Sintered Materials Based on Copper and Alumina Powders Synthesized by a Novel Method.

Kumar, C. A. V., & Rajadurai, J. S. (2016). Influence of rutile (TiO_2) content on wear and microhardness characteristics of aluminium-based hybrid composites synthesized by powder metallurgy. *Transactions of Nonferrous Metals Society of China (English Edition)*, *26*(1), 63–73.

Kumar, S., Srivatsan, T. S., & Gupta, M. (2007). Synthesis and mechanical behavior of carbon nanotube – magnesium composites hybridized with nanoparticles of alumina, *466*, 32–37.

Li, S., Kondoh, K., Imai, H., Chen, B., Jia, L., Umeda, J., & Fu, Y. (2016). Strengthening behavior of in situ -synthesized (TiC – TiB)/ Ti composites by powder metallurgy and hot extrusion. *JMADE*, *95*, 127–132.

Lin, H. Y., & Shih, C. Y. (2015). Efficient one-pot microwave-assisted hydrothermal synthesis of M (M = Cr, Ni, Cu, Nb) and nitrogen co-doped TiO_2 for hydrogen production by photocatalytic water splitting. *Journal of Molecular Catalysis A: Chemical*, *411*, 128–137.

Liu, J., Lin, L., Li, J., Liu, J., Yuan, Y., Ivanov, M., & Chen, M. (2014). Effects of ball milling time on microstructure evolution and optical transparency of Nd : YAG ceramics. *Ceramics International*, *40*(7), 9841–9851.

Low, I. M. (2014). *Advances in ceramic matrix composites: an introduction*. *Advances in ceramic matrix composites*. Woodhead Publishing Limited.

Mahani, Y. (2012). *Processing Microstructure and P Oroperties of In Situ Copper Reinforced Tungsten Carbide Nanostructured Composite*. University Science Malaysia.

Mahani, Y., & Zuhailawati, H. (2013). Effect of Compaction Pressure on Microstructure and Properties of Copper-Based Composite Prepared by Mechanical Alloying and Powder Metallurgy. *Advanced Materials Research*, *795*, 343–346.

Mahani Yusoff. (2012). *Processing, Microstructure and Properties of In Situ Copper Reinforced Tungsten Carbide Nanostructured Composite*.

Maria, A. B., Elias, S. U., Neto, P. F., & A. Pasa, A. (2015). Enhanced Photocatalytic Properties of Core@Shell SiO_2@TiO_2 Nanoparticles. *Applied Catalysis B: Environmental*, 1–42.

Meybodi, S. M., Barzegar Bafrooei, H., Ebadzadeh, T., & Tazike, M. (2013). Microstructure and mechanical properties of Al_2O_3–20wt%Al2TiO_5 composite prepared from alumina and titania nanopowders. *Ceramics International*, *39*(2), 977–982.

Minet, J., Langlais, F., Quenisset, J. M., & Naslaint, R. (1990). Thermomechanical Properties and Oxidation Resistance of Zirconia CVI-Matrix Composites : 1-- Mechanical Behavior, *5*(1989), 341–356.

Mishra, S. K., Gokuul, V., & Paswan, S. (2014). Int . Journal of Refractory Metals and Hard Materials Alumina-titanium diboride in situ composite by self-propagating high-temperature synthesis (SHS) dynamic compaction : Effect of compaction pressure during synthesis. *RMHM*, *43*, 19–24.

Nassar, A. E., & Nassar, E. E. (2015). Properties of Aluminum matrix Nano composites prepared by powder metallurgy processing. *Journal Of King Saud University - Engineering Sciences*.

Nenova, Z., Kozhukharov, S., Nenov, T., Nedev, N., & Machkova, M. (2016). Combined influence of titania and silica precursors on the properties of thin film humidity sensing elements prepared via a sol-gel method. *Sensors and Actuators, B: Chemical*, *224*, 143–152.

Ogawa, F., & Masuda, C. (2015). Microstructure Evolution during Fabrication and Microstructure – Property Relationships in Vapour-Grown Carbon Nanofibre-Reinforced Aluminium Matrix Composites Fabricated via Powder Metallurgy Kagami Memorial Institute for Materials Science and Technology. *Composite Part A*.

Ohnabe, H., Masaki, S., Onozuka, M., Miyahara, K., & Sasa, T. (1999). Potential application of ceramic matrix composites to aero-engine components. *Composites Part A: Applied Science and Manufacturing*, *30*(4), 489–496.

Oungkulsolmongkol, T., Salee-Art, P., & Buggakupta, W. (2010). Hardness and Fracture Toughness of Alumina-Based Particulate Composites with Zirconia and Strontia Additives. *Journal of Metals, Materials and Minerals*, *20*(2), 71–78.

Palmero, P., Kern, F., Sommer, F., Lombardi, M., Gadow, R., & Montanaro, L. (2014). Issues in nanocomposite ceramic engineering: focus on processing and properties of alumina-based composites. *Journal of Applied Biomaterials & Functional Materials*, *12*(3), 113–128.

Pournaderi, S., Mahdavi, S., & Akhlaghi, F. (2012). Fabrication of Al / Al 2 O 3 composites by in-situ powder metallurgy (IPM). *Powder Technology*, *229*, 276–284.

Powder, R., Techniques, M., & Miura, H. (2014). Advanced Powders Processing –, (82).

Qiu, F., Zuo, R., Shu, S. L., Wang, Y. W., & Jiang, Q. C. (2015). Effect of Al addition on the microstructures and compression properties of (TiCxNy-TiB_2)/Ni composites fabricated by combustion synthesis and hot press. *Powder Technology*, *286*, 716–721.

Rahimian, M., Parvin, N., & Ehsani, N. (2010). Investigation of particle size and amount of alumina on microstructure and mechanical properties of Al matrix composite made by powder metallurgy. *Materials Science and Engineering A*, *527*(4–5), 1031–1038.

Rocha-Rangel, E. (2013). Alumina-Based Composites Reinforced with Silver Particles. *Advances in Materials*, *2*(6), 62.

Rocha-rangel, E., Refugio garcia, E., Miranda-hernández, J., & Terres rojas, E. (2014). Alumina-based composites reinforced with silver particles, *2*(6), 62–65.

Rout, P. R. (2013). *A thesis submitted in partial fulfillment of the requirements for the degree of*. National Institute of Technology, Rourkela.

Sabzevari, M., Abdolkarim, S., & Moloodi, A. (2015). Physical and mechanical properties of porous copper nanocomposite produced by powder metallurgy. *Advanced Powder Technology*, 5–11.

Sakka, S., Bouaziz, J., & Ayed, F. Ben. (2014). Sintering and mechanical properties of the alumina – tricalcium phosphate – titania composites. *Materials Science & Engineering C*, *40*, 92–101.

Sanjay, M. R., Arpitha, G. R., & Yogesha, B. (2015). Study on Mechanical Properties of Natural - Glass Fibre Reinforced Polymer Hybrid Composites : A Review. *Materials Today: Proceedings*, *2*(4–5), 2959–2967.

Sekino, T., & Niihara, K. (1997). Fabrication and mechanical properties of fine-tungsten-dispersed alumina-based composites. *Journal of Material Science*, *2*, 3943–3949.

Sivakumar, S., Sibu, C. P., Mukundan, P., Pillai, P. K., & Warrier, K. G. K. (2004). Nanoporous titania – alumina mixed oxides — an alkoxide free sol – gel synthesis, *58*, 2664–2669.

Tahara, T., Imajyo, Y., Bayu, A., Nandiyanto, D., Ogi, T., & Iwaki, T. (2014). Low-energy bead-milling dispersions of rod-type titania nanoparticles and their optical properties. *Advanced Powder Technology*.

Thakur, S. K., Srivatsan, T. S., & Gupta, M. (2007). Synthesis and mechanical behavior of carbon nanotube-magnesium composites hybridized with nanoparticles of alumina. *Materials Science and Engineering A*, *466*(1–2), 32–37.

Thomas, S., Joseph, K., Malhotra, S. K., Goda, K., & Sreakala, M. S. (2012). Polymer Composites. In S. Thomas, K. Joseph, S. K. Malhotra, K. Goda, & M. S. Sreakala (Eds.), *Polymer Composite* (First edit, pp. 3–16). Germany: Wiley-VCH Verlag GmgH & Co. KGaA.

Vikas Somani. (2006). Alumina-Aluminum Titanate-Titania Nanocomposite : Synthesis , Sintering Studies , Assessment of Bioactivity and, 37–38.

Wang, W., Wang, M., Li, Z., Du, X., Xu, H., Zhao, W., … Ma, J. (2016). Scripta Materialia Synthesis and Characterization of Structural and Optical Properties of Heteroepitaxial Brookite TiO2 Single Crystalline Films. *Scripta Materialia*, *115*, 75–79.

Xiao, D. H., Yuan, T. C., Ou, X. Q., & He, Y. H. (2011). Microstructure and mechanical properties of powder metallurgy Ti-Al-Mo-V-Ag alloy. *Transactions of Nonferrous Metals Society of China (English Edition)*, *21*(6), 1269–1276.

Yan, T., & Wei, G. (2014). Multiscale Analysis of the Interfacial Mechanical Behavior for Composite of Carbon Nanotube and Alumina, *2014*.

Yang, Y., Wang, Y., Tian, W., Wang, Z., & Li, C. (2009). In situ porous alumina / aluminum titanate ceramic composite prepared by spark plasma sintering from nanostructured powders. *Scripta Materialia*, *60*(7), 578–581.

Yang, Y., Wang, Y., Tian, W., Zhao, Y., He, J. qi, Bian, H. min, & Wang, Z. qiang. (2009). In situ alumina/aluminum titanate bulk ceramic composites prepared by SPS from different structured composite powders. *Journal of Alloys and Compounds*, *481*(1–2), 858–862.

Yang, Y., Wang, Y., Wang, Z., Liu, G., & Tian, W. (2008). Preparation and sintering behaviour of nanostructured alumina/titania composite powders modified with nano-dopants. *Materials Science and Engineering A*, *490*(1–2), 457–464.

Yashwanth, I. V. S., & Gurrappa, I. (2015). The effect of titanium alloy composition in synthesis of Titania nanotubes. *Materials Letters*, *142*, 328–331.

Yavas, B., Sahin, F., Yucel, O., & Goller, G. (2015). Effect of particle size, heating rate and CNT addition on densification, microstructure and mechanical properties of B_4C ceramics. *Ceramics International*, *41*(7), 8936–8944.

Yavas, B., Sahin, F., Yucel, O., & Goller, G. (2015). Effect of particle size , heating rate and CNT addition on densi fi cation , microstructure and mechanical properties of B_4C ceramics. *Ceramics International*, 1–9.

Yin, W., Chen, S., Yang, J., Gong, X., Yan, Y., Yin, W., … Yan, Y. (2011). Effective band gap narrowing of anatase TiO_2 by strain along a soft crystal direction Effective band gap narrowing of anatase TiO_2 by strain along a soft crystal direction, *221901*(2010).

Zahedi, A. M., Javadpour, J., Rezaie, H. R., & Mazaheri, M. (2015). Author ' s Accepted Manuscript Analytical Study on the Incorporation of Zirconia- based Ceramics with Carbon Nanotubes : Dispersion Methods and Mechanical Properties Reference : To appear in : Ceramics International. *Ceramics International*.

Zainudin, E. S., & Sapuan, S. M. (2009). Multidiscipline Modeling in Materials and Structures Article information : Banana Pseudo-Stem Filled Unplastisized PVC. *Multidiscipline Modeling in Materials and Structures*, *5*(3), 277–282.

Zeng, X., Liu, Y., Huang, Q., Zeng, G., & Zhou, G. (2013). Materials Science & Engineering A Effects of carbon nanotubes on the microstructure and mechanical properties of the wrought Mg –2.0Zn alloy. *Materials Science & Engineering A*, *571*, 150–154.

Zhao, J. (2014). *The use of ceramic matrix composites for metal cutting applications*. *Advances in Ceramic Matrix Composites*. Woodhead Publishing Limited.

Zuhailawati, H., & Mahani, Y. (2009). Effects of milling time on hardness and electrical conductivity of in situ Cu–NbC composite produced by mechanical alloying, *476*, 142–146.

APPENDIX A

CALCULATIONS

A.1 Calculation of Change Mpa to Tons for Compaction Samples

Example change of 200 MPA to unit of Tons, the changes can be calculated from

P = 200 MPa, d= 10 mm, r= 5 mm

$P = \frac{F}{A}$

$F = P(\pi r^2)$

$F = 200\ (3.142)(5)^2$

$= \frac{1.57E4}{9.81}$

$= \frac{1600.41}{1000}$

$= 1.60$

A.2 Example of Green Density for 15 Hours of Powder Milled

$GD = \frac{mass}{volume}$

$GD = \frac{1.104}{0.424}$

$GD = 2.604\ gcm^{-1}$

A.3 Example of Densification Parameter for 15 Hours of Powder Milled

$\text{Densification parameter} = \frac{GD-AD}{TD-AD}$

$DP = \frac{2.594-0.772}{3.980-0.772}$

$DP = 0.568$

APPENDIX B

TABLES

B.1 Pellet Sample Of Al_2O_3-TiO_2-CNT composite

a) 15 h

Pressure (MPa)	Width (mm)		Weight (g)		Average width	Average weight
	Sample 1	Sample 2	Sample 1	Sample 2		
200	5.23	5.26	1.086	1.093	5.25	1.090
400	4.98	5.11	1.089	1.087	5.05	1.088
600	4.94	5.09	1.088	1.089	5.02	1.089
800	4.90	4.88	1.084	1.085	4.89	1.085

b) 30 h

Pressure (MPa)	Width (mm)		Weight (g)		Average width	Average weight
	Sample 1	Sample 2	Sample 1	Sample 2		
200	5.23	5.38	1.104	1.083	5.31	1.094
400	5.07	4.97	1.101	1.085	5.02	1.093
600	5.02	4.75	1.107	1.082	4.89	1.095
800	4.77	4.74	1.094	1.089	4.76	1.092

c) 45 h

Pressure (MPa)	Width (mm)		Weight (g)		Average width	Average weight
	Sample 1	Sample 2	Sample 1	Sample 2		
200	5.53	5.27	1.086	1.093	5.25	1.090
400	4.96	5.09	1.089	1.087	5.05	1.088
600	4.86	4.87	1.088	1.089	5.02	1.089
800	4.79	4.65	1.084	1.085	4.89	1.085

d) 60 h

Pressure (MPa)	Width (mm)		Weight (g)		Average width	Average weight
	Sample 1	Sample 2	Sample 1	Sample 2		
200	5.23	5.26	1.086	1.093	5.25	1.090
400	4.98	5.11	1.089	1.087	5.05	1.088
600	4.94	5.09	1.088	1.089	5.02	1.089
800	4.90	4.88	1.084	1.085	4.89	1.085

B.2 Green Density

Pressure	15 h	30 h	45 h	60 h
200	2.594	2.559	2.528	2.615
400	2.688	2.559	2.762	2.677
600	2.714	2.559	2.838	2.757
800	2.764	2.559	2.895	2.837

B.3 Densification Parameter

Pressure	15 h	30 h	45 h	60 h
200	0.568	0.568	0.548	0.579
400	0.597	0.610	0.621	0.598
600	0.605	0.632	0.645	0.622
800	0.621	0.649	0.663	0.647

B.4 Apparent density

Milling Time	Mass	Volume	Apparent Density
15	5.266	6.817	0.772
30	5.335	6.817	0.782
45	5.218	6.817	0.720
60	4.909	6.817	0.739

APPENDIX C

FIGURE

C.1 Pure powder

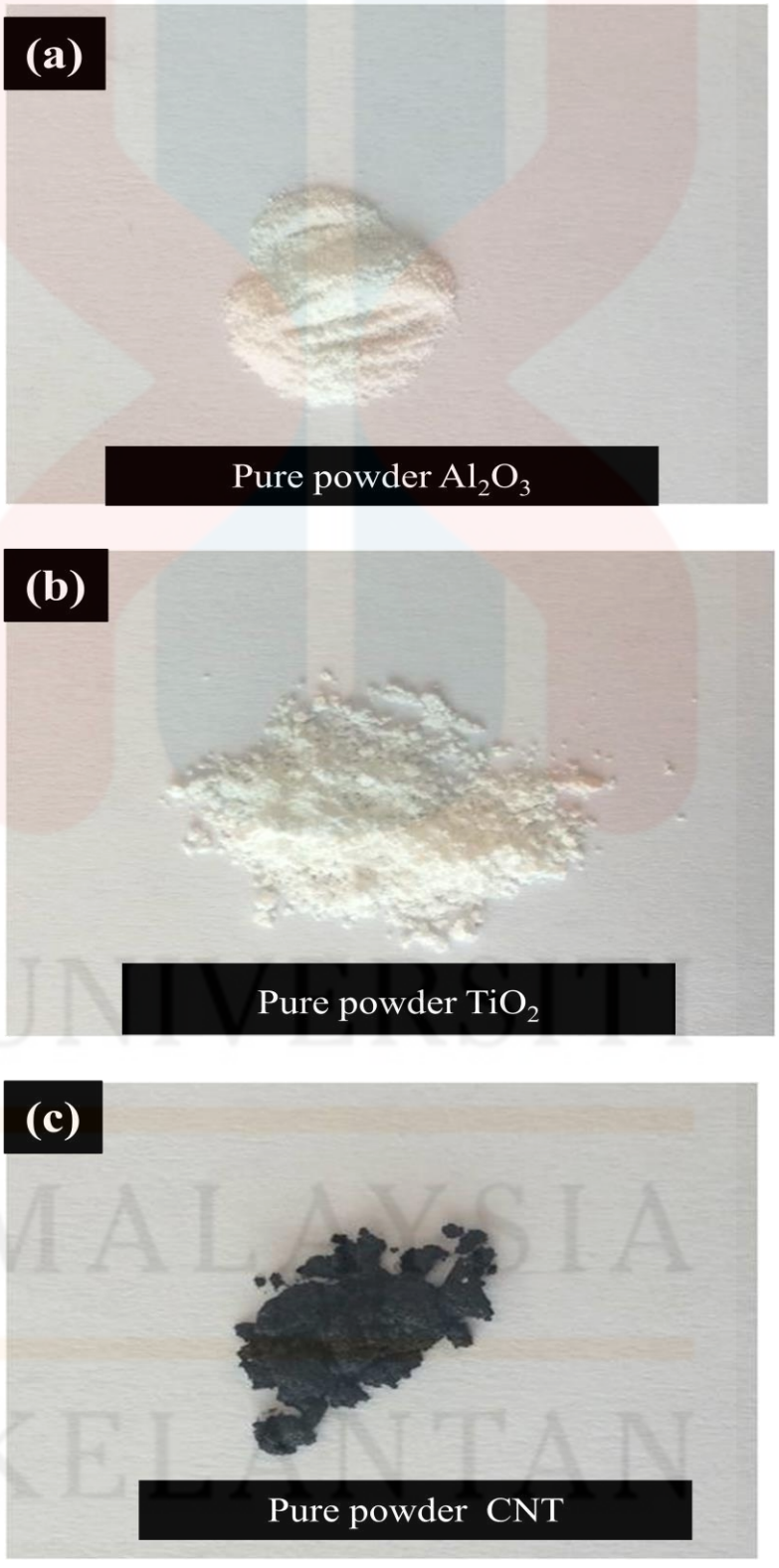

C.2 Milled Powder

C.3 Al_2O_3–TiO_2–CNT composite

C.4 Example of Uniaxial Hand Pressing